

Stochastic ground motion method combining a
Fourier amplitude spectrum model from a
response spectrum with application of phase
derivatives distribution prediction

Marco Baglio, Norman Abrahamson, Gian Paolo Cimellaro

November 27, 2017

Abstract

A simple method based on creation of Fourier amplitude spectrum model from a response spectrum is presented. The procedure generates suites of stochastic ground motions strictly matching the mean value of a target response spectrum. The application of white-noise with constraints on the variance and inter-frequency correlation provides the realistic variability of the Fourier amplitude spectrum. A two corner frequency model is estimated from empirical ground-motion data and a kappa filter is applied to capture the attenuation at high frequencies. The method showed excellent matching in terms of both the mean and dispersion values with either the median from GMPEs or conditional mean spectra. Time-histories generated by this methodology do not require scaling or frequency content adjustments. The method proposed can be successfully applied from Design spectra.

Phase derivatives distributions of the PEER NGA-West1 database are estimated and the relationship between the distribution dispersion and seismological parameters are evaluated. The shape parameter of logistic distribution is proposed as an appropriate measure of dispersion of the phase derivative. First, the relation between the shape parameter and the significant duration (5-75% Arias intensity) is used to check database for outliers. Second, an empirical relation relating shape parameter with moment magnitude, rupture distance, soil category and rupture directivity is developed using non-linear regression. Three applications of the phase derivative models for stochastic ground motion models are proposed: (i) random logistic-distributed phase angles, (ii) calibration of an exponential time window consistent with the phase derivatives shape parameter, and (iii) generation of a near fault pulses using a modified phase difference distribution.

The stochastic ground motions generation is used to develop suite of time

histories for the conditional scenario spectra (CSS). The CSS are a set of response spectra with assigned rates of occurrence that reproduce the hazard over a wide range of hazard levels and spectral periods at one site. The CSS provide an estimate of the seismic history for a site in terms of the time histories likely to be experienced at the site. These time histories and their rates are then used to estimate the hazard curve for engineering demand parameters. The method used for generate stochastic ground motions is based on matching target response spectra which is the main set of CSS. The main advantages of this application are: (i) the small number of time histories (generally less than one hundred) required to reproduce the hazard compared to methods that use recorded time histories, and (ii) the very fast computation.

Acknowledgements

I would like to express my gratitude to my advisor, Professor Norman Abrahamson, for his precious support; he led me through the work presented in this paper by patiently introducing me into notions necessary to study in deep all the discussed topics. Other thanks are directed to my supervisors Professor Gian Paolo Cimellaro and Professor Stephen Mahin, I had the possibility to study and work on my thesis at the University of Berkeley only thanks to them; they followed me during my studies providing advice and help in every situation.

Ringraziamenti

Vorrei ringraziare la mia famiglia per essermi sempre stata vicino nel corso dei miei studi universitari (e non solo). Pronti a gioire con me dei miei successi così come ad incoraggiarmi e spronarmi nei momenti di difficoltà (che non sono stati pochi). Nell'ultimo periodo le difficoltà sono aumentate, ma voi avete continuato a supportarmi senza farmi mancare nulla. La mia forza siete voi.

Contents

Abstract	i
Acknowledgements	iii
Ringraziamenti	iv
1 Introduction	2
2 Stochastic ground motion model	5
2.1 Abstract	5
2.2 Introduction	6
2.3 Fitted FAS model	7
2.4 Comparison with GMPEs and CMS	11
2.5 Interfrequency correlation	18
2.6 Application from a design spectrum	21
2.7 Conclusions	22
3 Analysis of phase derivatives distribution and application for stochastic ground motions	23
3.1 Abstract	23
3.2 Introduction	24
3.3 Phase angles processing and probability density functions . . .	25
3.4 Model definition	27
3.5 Regression analysis	29
3.5.1 First stage	29
3.5.2 Second stage	29
3.5.3 Third stage	32

3.6	Applications	34
3.6.1	Random logistic-distributed phase derivatives	34
3.6.2	Exponential window calibration	35
3.6.3	Pulse creation	37
3.7	Conclusions	39
4	Conditional scenario spectra generation through simulated spectra	41
4.1	Abstract	41
4.2	Introduction	42
4.3	Conditional Scenario Spectra definition	43
4.4	Procedure of CSS creation	44
4.4.1	GMPEs generation	44
4.4.2	Scenario spectra selection	45
4.4.3	Rates of occurrence calibration	48
4.4.4	Summary	50
4.5	Conclusions	54
5	Conclusions	56
5.1	Fourier amplitude spectrum model	56
5.2	Phase derivatives analysis	58
5.3	Conditional scenario spectra through simulated spectra	59

List of Figures

2.1	Description of white-noise generation and scaling.	8
2.2	Response spectra and Fourier amplitude spectra of the adjusted samples.	9
2.3	GMPE and CMS along with fitted FAS model for the Francofonte example site. Uniform hazard spectrum comes from Italian interactive seismic hazard map.	12
2.4	$f_{a,\varepsilon}$ solution pairs for each FAS model.	13
2.5	Suite of simulated spectra for each target.	15
2.6	Goodness of fit plots. The black line is mean bias, light gray shading shows its standard deviation and dark shading shows 90% confidence limits on the mean bias.	16
2.7	Logarithmic standard deviation plots for each target spectrum.	17
2.8	Comparison between simulated correlation (left column) and model correlation (right column) for FAS and spectral acceleration values.	19
2.9	Spectral acceleration correlation for periods 0.2 s , 0.5 s and 1 s	20
2.10	Suite of stochastic ground motions matching Eurocode 8 design spectrum. κ filter is set to 0.08 s , logarithmic standard deviation σ to 1	21
3.1	ChiChi earthquake record and its phase derivatives.	26
3.2	First stage regression plots.	29
3.3	First stage residuals quantile-quantile plot.	30
3.4	ChiChi earthquake record. This is an example of record removed from regression analysis.	31

3.5	Logarithmic residuals versus magnitude, rupture distance and soil category.	32
3.6	Second stage residuals quantile-quantile plot.	33
3.7	Stochastic ground motion generated by random logistic-distributed phase derivatives.	35
3.8	Comparison between a suite of real ground motions and stochastic ground motions in terms of Arias intensity. Time zero is set at 50% of Arias intensity.	36
3.9	Regression lines expressing the relationship between signal total duration and phase derivatives shape parameters.	37
3.10	Acceleration, phase differences, velocity and displacement of a stochastic ground motion generated by exponential window phase angles. The record contains a velocity pulse created by centering phase differences below 1 Hz	38
4.1	Uniform hazard spectra in Francofonte, Sicily.	44
4.2	Representation of only GMPEs calibrated for the first and last hazard levels along with the Uniform hazard spectra (dotted line).	46
4.3	Set of candidate scenario spectra computed for each hazard level.	47
4.4	Plot of normalized residuals for each hazard level. In first graph, gray lines represent the normalized residuals for each scenario spectrum, red line represent the mean value. In second graph, black line represent the standard deviation of normalized residuals. Montecarlo simulation aims to match red line with θ and black line with 1	49
4.5	Comparison of spectral values correlation. Montecarlo simulation aims to match the correlation represented in the first plot with the second plot.	50

4.6	Comparison between target and hazard estimated from CSS for periods $0.15 s$ and $1.5 s$ before and after optimization. Application of weighted misfit provides better matching at high levels hazard trading off for a reduction of matching at low hazard levels.	51
4.7	Comparison between target UHS and recovered by Conditional scenario spectra UHS.	52
4.8	CSS and rates of occurrence for the case study of Francofonte, Sicily.	52

List of Tables

2.1	Parameters used in GMPEs computation. Omitted values are set as unknown.	14
3.1	First and second stage parameters.	30
3.2	Second stage correlation matrix.	31
3.3	Parameters obtained by third stage regression.	33
3.4	Third stage correlation matrix.	33
4.1	Mean values of magnitude and distance for different return periods in Francofonte, Sicily.	45

Chapter 1

Introduction

Dynamic structural analysis is increasingly advancing into selection of real ground motions as input; records databases and reliability are constant growing, moving artificial ground motions to the background. Nevertheless, these databases does not totally cover all areas of the world as well as case studies with high magnitude earthquakes; therefore real records are not suffice and other resources are needed.

Douglas, Aochi (2008) proposes a survey of all methodologies used to generate predicted earthquakes ground motions. Overall, it is possible to divide all the methodologies in two approaches: 'physics-based' and experimental approach. The first one can be defined as mathematical models based on physical principles; the second one as mathematical models based on fitting of experimental data.

The second category is also named 'black box' method, because it is based on the recreation of a certain feature of ground motion records without physical considerations. A common method is the usage of white noise modified by filtering in the frequency domain and multiplied by an envelope function. Usually, the frequency content and envelope function are obtained by prediction equations (Sabetta, Pugliese, 1996). SIMQKE (Gasparini, Vanmarcke, 1976) is another code belonging to this category; the frequency content is filtered by a function which is obtained from a target elastic response spectrum. Furthermore, the latter requires an iterative process of adjustment in the frequency content.

The lack of physic assumptions in the 'black box' methods moved the focus of researchers in the first category, where it is possible to find a larger number of solutions. Boore (2003) proposes one of the most exhaustive and simple 'physic-based' methods. A Fourier amplitude spectrum (FAS) model is estimated using a point-source spectrum model; therefore, this is transferred to the site by means of anelastic and geometric attenuation. The obtained FAS is used for filtering a Gaussian white noise by following the same procedure of 'black box' category. Natural prosecution of this method is the discretization of the complex geometry of a fault by the combination of several points-source spectra. Atkinson, Assatourians (2015) describes the implementation and validation of such methodology.

Another group of physic-based methods is composed by finite difference methods (FDM), finite element methods (FEM) and spectral element methods (SEM). They are becoming more and more the best solution for simulate near-fault effect and obtain a reliable prediction of an earthquake source location and information about the medium. Drawbacks are the very high time consumption and the difficulties to parallelize the computation.

In chapter 2 is proposed a methodology which fits in the physic-based category. The work-flow is coincident with the procedure used in Boore (2003): the frequency content of white noise is filtered by a FAS model and inverted in the time domain. First novelty consists of a procedure for obtain a FAS model from a target response spectrum. The FAS model is developed by means of a generalized double corner frequency model and application of an high-frequency filter commonly used for stochastic ground motions. Second novelty comes from the achievement of time non-stationarity. Typically, the white noise is windowed by an envelope function in the time domain and then filtered in the frequency domain. The effect of such windowing is represented in the frequency domain by a variation of phase derivatives (the derivative of phase angles) distribution. For this aim, in chapter 3 a study of earthquakes phase derivatives is presented in order to propose a prediction equation to apply for stochastic ground motions non-stationarity. This methodology allows the creation of suites of stochastic ground motions able to have a mean values matching a target response spectrum. Furthermore, the FAS is generated by means of a covariance matrix; this leads to two remarkable improvements, (i)

dispersion consistent with the target spectrum obtained by the adjustment in the variance and (ii) inter-frequency correlation consistent with earthquakes records.

In summary, suites of stochastic ground motions generated by this procedure show mean value and dispersion consistent with a target spectrum and correlation in the frequency content. Moreover, the application of phase derivatives ad hoc computed according to site conditions provides congruous time non-stationarity. All these features allows the application of stochastic ground motions for the generation of Conditional Scenario Spectra (CSS). The CSS is a selection of response spectra with assigned rates of occurrence, which is able to represent all the seismic scenarios for a case study. Therefore, such set can be used to obtain fragility curve of engineering demand parameters (EDP); in other words, a plot of the variation of a meaningful parameter (e.g. interstory drift) according to the hazard level. The inputs are the Uniform hazard spectra with an assigned hazard and mean value of magnitude and distance for each level. Chapter 4 describes in detail the procedure to develop the CSS from stochastic ground motions.

Chapter 2

Stochastic ground motion model

2.1 Abstract

A simple method based on creation of Fourier amplitude spectrum model from a response spectrum is presented. The procedure generates suites of stochastic ground motions strictly matching the mean value of a target response spectrum. The application of white-noise with constraints on the variance and inter-frequency correlation provides the realistic variability of the Fourier amplitude spectrum. A two corner frequency model is estimated from empirical ground-motion data and a kappa filter is applied to capture the attenuation at high frequencies. The method showed excellent matching in terms of both the mean and dispersion values with either the median from GMPEs or conditional mean spectra. Time-histories generated by this methodology do not require scaling or frequency content adjustments. The method proposed can be successfully applied from Design spectra.

2.2 Introduction

A relationship between a response spectrum and the Fourier amplitude spectrum (FAS) was proposed in Gasparini, Vanmarcke (1976). The aim is achieved by the application of random vibration theory which provides the power spectral density function definition from a response spectrum by an iterative process. FAS is obtained by energetic equilibrium with the power spectral density function. Therefore, time-histories are computed as superposition of sine waves shaped by an envelope function to accomplish the non-stationarity. FAS models from this method often show unphysical trends in low and high frequency ranges and require a final process of scaling to match the response spectrum. A process of adjustment in the frequency domain is necessary to improve the spectrum matching. Herein, a method to define a FAS model based on physical constraints is proposed. The procedure aims to obtain a FAS model that allow the creation of stochastic ground motions which response spectra are consistent with a target spectrum. Moreover, the application of inter-frequency correlation model provides the generation of FAS with proper variability and correlation. No scaling and adjustment is required to this methodology.

2.3 Fitted FAS model

The method is based on the generation of a FAS model from a target response spectrum. Equation 2.1 represents the generalized FAS model used to recreate the frequency amplitudes in the low frequency range.

$$FA(C, f_a, \varepsilon, f) = C \left[\frac{f^2(1 - \varepsilon)}{1 + \left(\frac{f}{f_a}\right)^2} + \frac{f^2\varepsilon}{1 + \frac{f^2}{(f_c^2 - f_a^2)/\varepsilon + f_a^2}} \right] \quad (2.1)$$

It is an additive double corner frequency ($f_a; f_b$) model (D. M. Boore, Abrahamson, 2014); ε is a weighting parameter giving the relative contributions of the two spectra, C is a scaling parameter. The expression is obtained by the constraint of flat high-frequency acceleration spectrum and equating the double corner frequencies model to the single corner frequency model:

$$f_b = f_a \sqrt{\frac{(f_c/f_a)^2 - (1 - \varepsilon)}{\varepsilon}} \quad (2.2)$$

Attenuation at high frequencies is modeled by the application of κ filter (Anderson, Hough, 1984), which is multiplied by the equation 2.1.

$$D(f) = e^{-\pi\kappa f} \quad (2.3)$$

Following a procedure aiming to find ε , f_a and C calibrated for matching low frequency part of the target response spectrum and a proper value of κ for the high frequency part:

1. A target spectrum is developed. It can be computed from either GMPE or conditional mean spectrum. A value of magnitude is set.
2. Twenty samples of white-noise are generated. No time window is applied. The duration should be no less than 10 s in order to provide sufficient frequency resolution. FAS of each sample is scaled by the ω -square model (Aki, 1967) expressed in eq. 2.4. The corner frequency value (f_c) is set from the magnitude chosen in the first step¹.

$$FA = \frac{2\pi f^2}{1 + \left(\frac{f}{f_c}\right)^2} \quad (2.4)$$

This step is represented in figure 2.1.

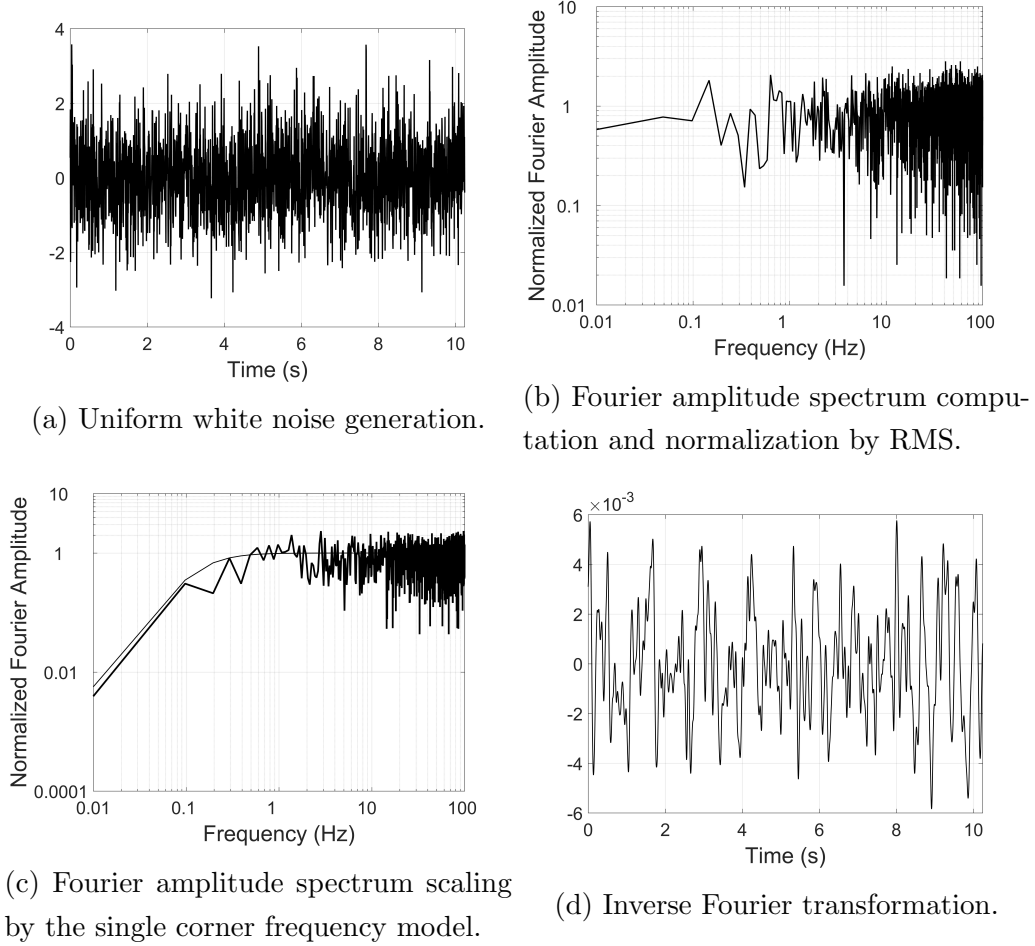


Figure 2.1: Description of white-noise generation and scaling.

- Four cycles of adjustment are performed in the frequency domain (FA_i) proportionally to the response spectrum mismatching (SA_T/SA_i) to obtain a strict spectrum-matching (see figure 2.2a):

$$FA_{i+1} = FA_i \frac{SA_T}{SA_i} \quad (2.5)$$

- The combined suite of samples is fit with the model in equation 2.1.

¹In our applications the corner frequency is computed by $\log(f_c) = 2.623 - 0.5M$

Non-linear regression estimates ε , f_a and C (see figure 2.2b); f_c is fixed by the single corner frequency model.

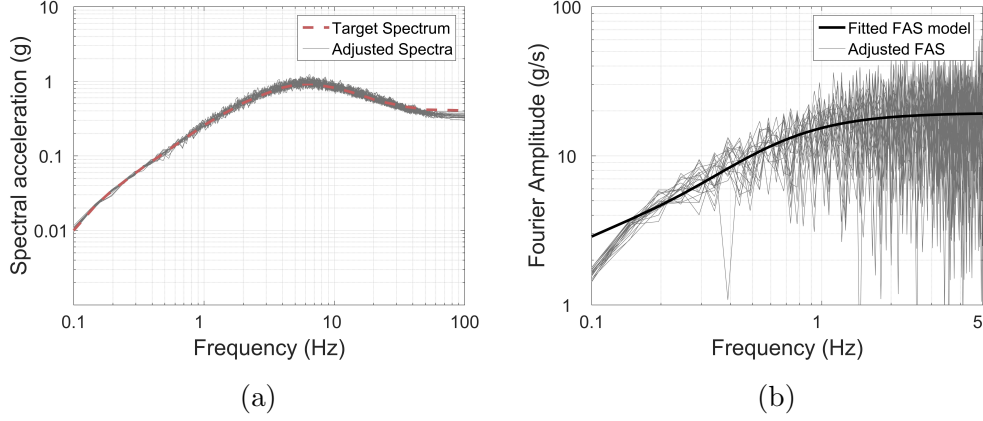


Figure 2.2: Response spectra and Fourier amplitude spectra of the adjusted samples.

5. A large number of realizations (e.g. 1000) is generated from the FAS model with ε , f_a and C estimated in the previous step. κ filter is applied with a value of 0.03 s. The procedure of generation can be summarized as follow:

- Random Fourier amplitudes ($\ln A(f)$) computation according to a multivariate normal distribution (Stafford, 2017) with mean vector $FA(C, f_a, \varepsilon, f_c, f)$ and covariance matrix $\Sigma(f)$:

$$\ln A(f) \sim N[FA(C, f_a, \varepsilon, f_c, f), \Sigma(f)] \quad (2.6)$$

- Random uniform phase angles generation. During this step, phase angles are generated uniform because the aim is to carry out a fast computation and the non-stationarity of each realization is not necessary.
- Inverse Fourier transform computation to obtain the simulated accelerograms.

6. Computation of response spectrum for each realization. Therefore computation of mean response spectrum.

7. Visual check if the mean response spectrum matches the target spectrum in short periods. If an adequate matching is not obtained, the procedure go back to step 5 and κ is adjusted. This part is repeated until short periods matching is guaranteed.
8. Eventually time-histories can be obtained from the FAS model with ε , f_a and C estimated in step 4 and κ value from the previous step. The procedure of generation is equivalent to the one described in step 5 with the application of a proper distribution of phase angles:
 - Random Fourier amplitudes ($\ln A(f)$) computation according to a multivariate normal distribution (Stafford, 2017) with mean vector $FA(C, f_a, \varepsilon, f_c, f)$ and covariance matrix $\Sigma(f)$ (see eq. 2.6).
 - Phase angles computation by procedure proposed in chapter 3.
 - Inverse Fourier transform computation to obtain the simulated accelerograms.

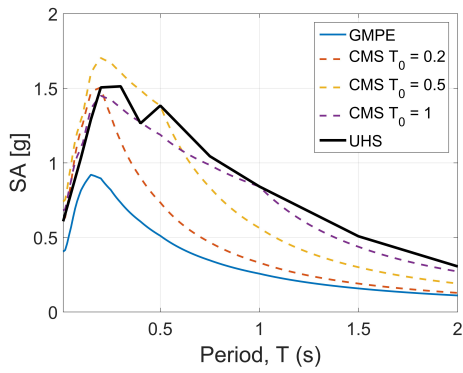
2.4 Comparison with GMPEs and CMS

The method is tested with four target spectra. Geometric mean [0.22ASK 0.22BSSA 0.22CB 0.22CY 0.12IM] of NGA-West2 equations (N. A. Abrahamson, Kamai, 2014; D. M. Boore, Atkinson, 2014; Campbell, Bozorgnia, 2014; Chiou, Youngs, 2014; Idriss, 2014) is developed; table 2.1 shows GMPEs input. Parameters are selected according to site conditions of Francofonte, Sicily; a set of conditional mean spectra is created from the GMPE by conditioning to site uniform hazard spectrum (2475 years return period) at structural periods 0.2, 0.5 and 1 seconds. Figure 2.3a shows the four spectra. We set a procedure for each target spectrum based on the following steps:

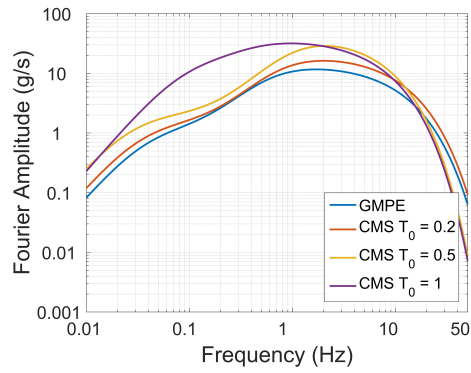
- Obtain FAS model parameters and $kappa$ by the procedure previously described.
- Generate a suite of 1000 stochastic ground motions. Random logistic-distributed phase angles are used (see chapter 3) for obtain non-stationarity. Each time-history is baseline corrected and low-filtered by Butterworth filter with a cut-off frequency of 0.02 Hz.
- (Exclusively for CMS) Remove each time-history exceeding the mean target value +/- 2.5 times the standard deviation. Logarithmic standard deviation is limited at 0.15 for avoid "pinch" in the conditioning period.

Figure 2.3b shows FAS models obtained. Overall, FAS models represent consistency with target spectra; in particular, 1 s CMS highlights the model flexibility, that is able to reproduce higher amplitudes at low frequencies. FAS model parameters computation includes a multivariable analysis, considering three outputs. Figure 2.4 represent the region of possible f_a, ε pairs (C is fixed) shaded according to the coefficient of determination R^2 . In our applications best pairs (in terms of R^2) are far from f_{lim} frontier (i.e. f_a upper bound, see eq. 2.7) with ε value around 0.1.

$$f_{lim} = \sqrt{\frac{1}{1 - \varepsilon}} f_c \quad (2.7)$$



(a) Target spectra.



(b) Fitted FAS models.

Figure 2.3: GMPE and CMS along with fitted FAS model for the Francofonte example site. Uniform hazard spectrum comes from Italian interactive seismic hazard map.

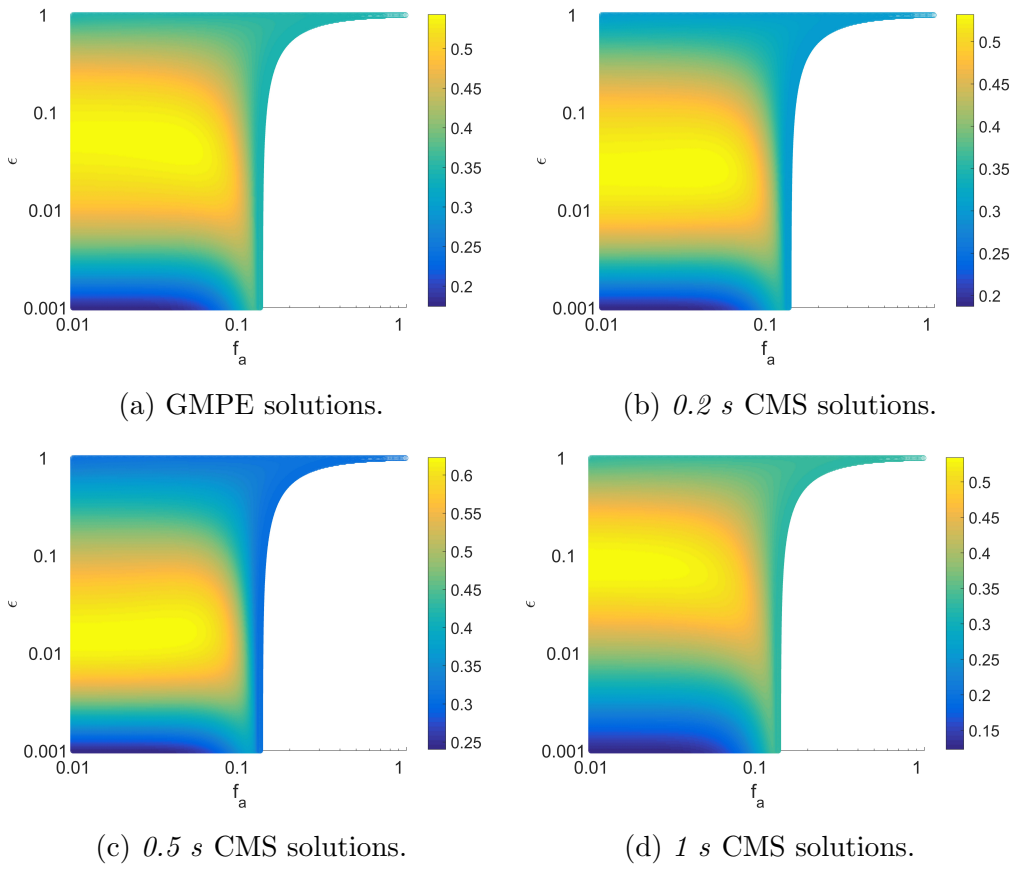


Figure 2.4: f_a, ϵ solution pairs for each FAS model.

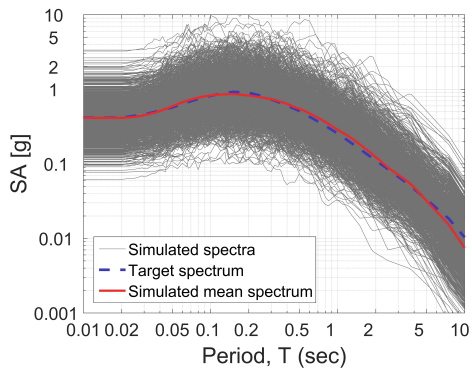
Table 2.1: Parameters used in GMPEs computation. Omitted values are set as unknown.

M	R_{rup} (km)	R_{jb} (km)	R_x (km)	R_{y0} (km)	V_{s30} (m/s)	F_{rv}	F_{nm}	F_{hw}	Dip (°)	Z_{tor} (km)
7	6	4.47	-4.47	0	760	1	0	0	45	4

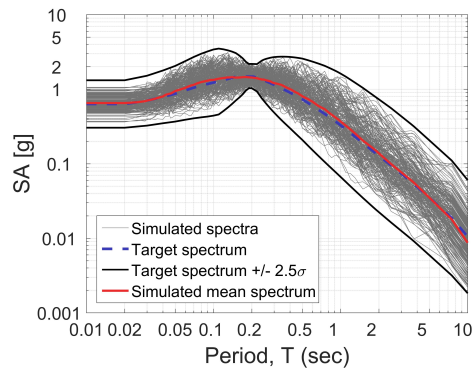
Figure 2.5 shows suites of spectra for each target. A perfect matching of the mean value can be considered in range between $0.01 s$ and $10 s$ as confirmed by Goodness of fit plot (see figure 2.6) with logarithmic residuals lying within a range of ± 0.2 .

A measure of dispersion is produced through the comparison of standard deviation between target spectrum and simulated spectra. Concerning the variance of input FAS (i.e. the variance used in the eq. 2.6), it is important to remark that in these applications we fixed the variance to a constant value of 0.8 . Such imposition allows to recreate a dispersion consistent with the GMPE standard deviation as showed by figure 2.7a. However, the comparison with CMS standard deviation showed a general underestimation of dispersion when distant from conditioning period.

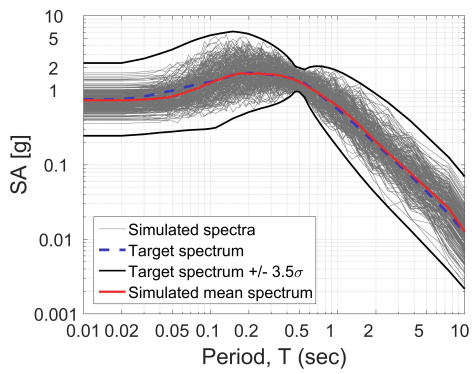
It is intuitive that such behavior is governed by the inter-frequency correlation model implemented for the generation of FAS, some considerations about the correlation are presented in the next section.



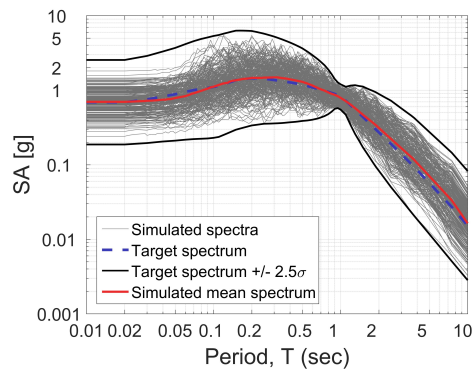
(a) GMPE.



(b) 0.2 s CMS.

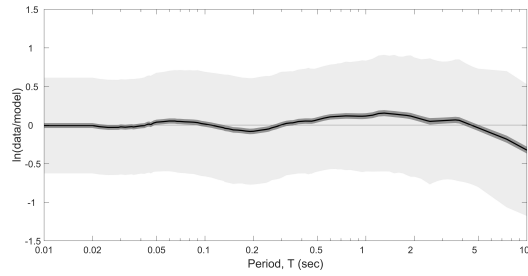


(c) 0.5 s CMS.

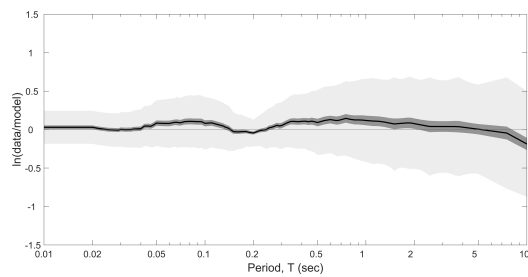


(d) 1 s CMS.

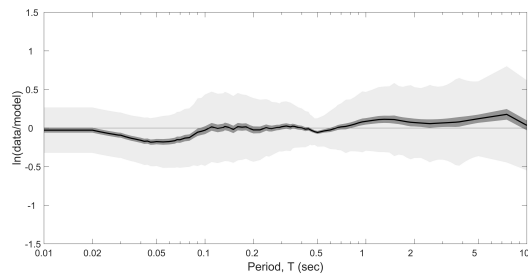
Figure 2.5: Suite of simulated spectra for each target.



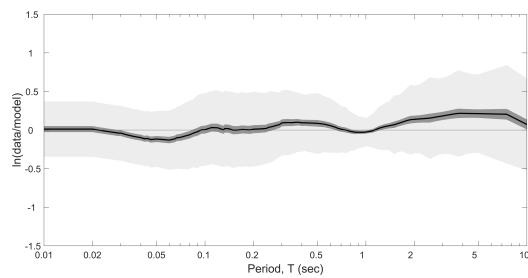
(a) GMPE goodness of fit.



(b) *0.2 s* CMS goodness of fit.

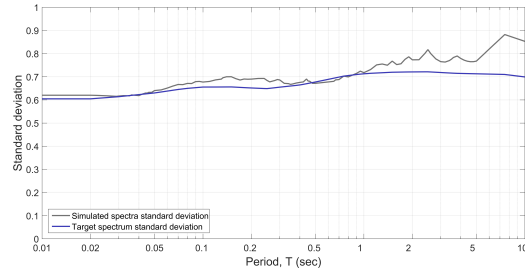


(c) *0.5 s* CMS goodness of fit.

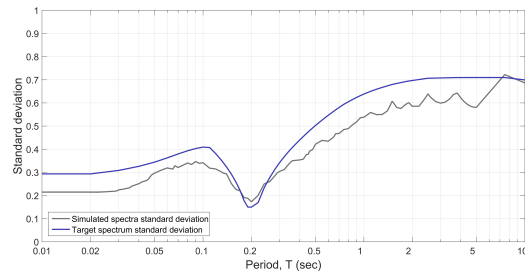


(d) *1 s* CMS goodness of fit.

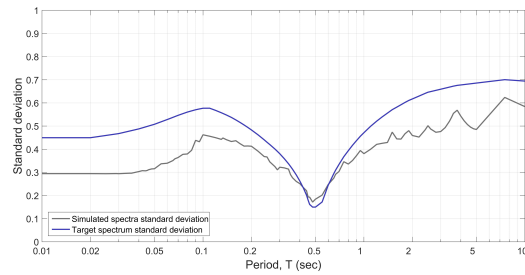
Figure 2.6: Goodness of fit plots. The black line is mean bias, light gray shading shows its standard deviation and dark shading shows 90% confidence limits on the mean bias.



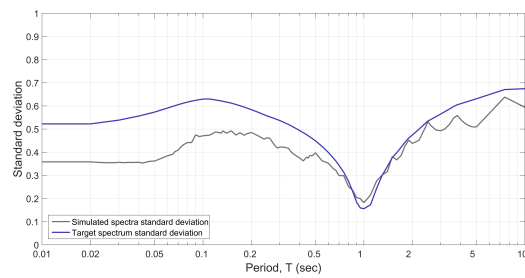
(a) GMPE standard deviation.



(b) 0.2 s CMS standard deviation.



(c) 0.5 s CMS standard deviation.



(d) 1 s CMS standard deviation.

Figure 2.7: Logarithmic standard deviation plots for each target spectrum.

2.5 Interfrequency correlation

The model proposed in Stafford (2017) is used in the generation of stochastic ground motions with inter-frequency correlation (see eq. 2.6):

$$\ln A(f) \sim N[FA(C, f_a, \varepsilon, f_c, f), \sum(f)] \quad (2.8)$$

The mean vector $FA(C, f_a, \varepsilon, f_c, f)$ is defined has been defined previously. The Covariance matrix $\sum(f)$ is expressed as follow:

$$\sum(f) = \begin{bmatrix} \sigma^2(f_1) & \rho(f_1, f_2)\sigma(f_1)\sigma(f_2) & \cdots & \rho(f_1, f_n)\sigma(f_1)\sigma(f_n) \\ \rho(f_2, f_1)\sigma(f_2)\sigma(f_1) & \sigma^2(f_2) & \cdots & \rho(f_2, f_n)\sigma(f_2)\sigma(f_n) \\ \vdots & \vdots & \ddots & \vdots \\ \rho(f_n, f_1)\sigma(f_n)\sigma(f_1) & \rho(f_n, f_2)\sigma(f_1)\sigma(f_2) & \cdots & \sigma^2(f_n) \end{bmatrix} \quad (2.9)$$

Where $\sigma(f_i)$ is the standard deviation at the frequency f_i and $\rho(f_i, f_j)$ is the correlation between frequencies f_i and f_j . They come from three different contributions; between-event component (E), within-event component (A) and between-site component (S):

$$\rho(f_i, f_j) = \frac{\rho_E(f_i, f_j)\sigma_E(f_i)\sigma_E(f_j) + \rho_A(f_i, f_j)\sigma_A(f_i)\sigma_A(f_j) + \rho_S(f_i, f_j)\sigma_S(f_i)\sigma_S(f_j)}{\sigma(f_i)\sigma(f_j)} \quad (2.10)$$

$$\sigma^2(f_i) = \sigma_E^2(f_i) + \sigma_A^2(f_i) + \sigma_S^2(f_i) \quad (2.11)$$

Each contribution is defined in Stafford (2017).

A test was carried out on the suite of one thousand simulated spectra from GMPE, in order to check the consistency of correlation obtained by this methodology. Figure 2.8a shows the correlation computed from logarithmic residuals of FAS model. A visual check with the imposed correlation model in figure 2.8b confirms the generation of inter-frequency correlation in the FAS.

A further test on spectral acceleration correlation was performed with the model proposed by Baker, Jayaram (2008) and corrected in the high frequency part according to Carlton, Abrahamson (2014) (0.05 s is the $T_{1.5}$ from the target GMPE) represented in figure 2.8d. The correlation obtained by the suite is plotted in figure 2.8c. It shows consistency in the shape,

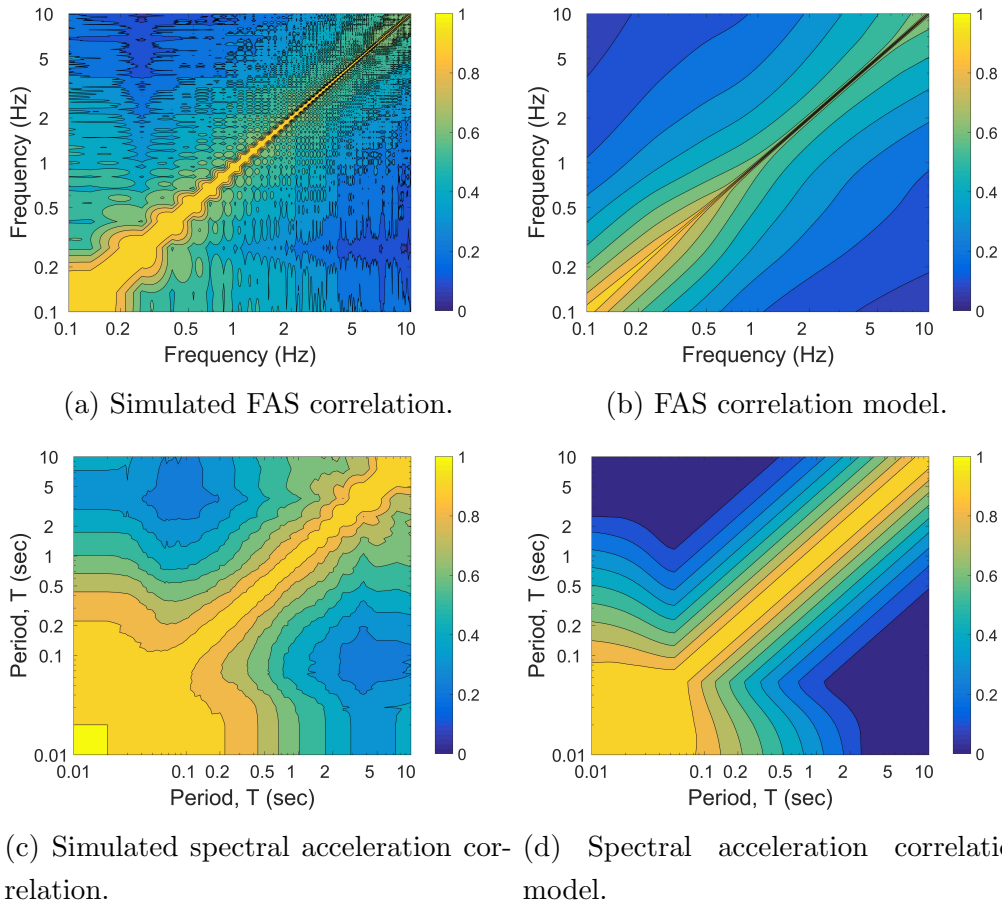


Figure 2.8: Comparison between simulated correlation (left column) and model correlation (right column) for FAS and spectral acceleration values.

although a general overestimation is detected, especially in short periods (see fig. 4.5). Such difference is behind the underestimation of dispersion obtained from CMS; namely, the standard deviation is more correlated to the conditioning period than the model in Baker, Jayaram (2008).

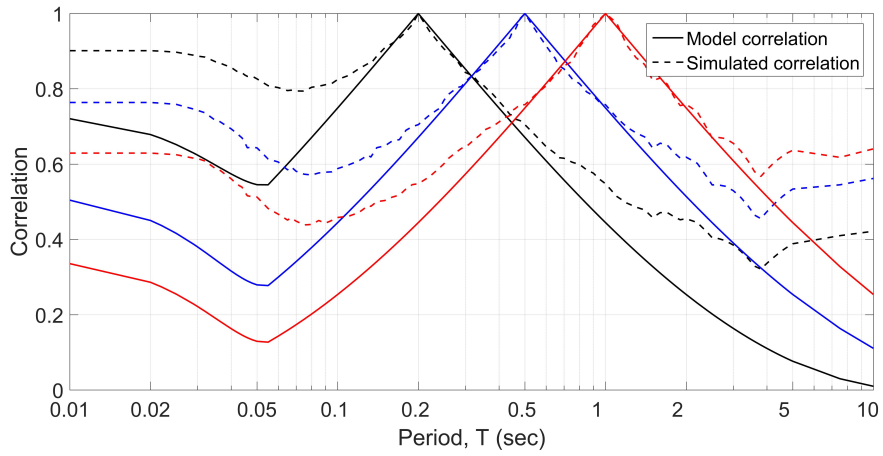


Figure 2.9: Spectral acceleration correlation for periods 0.2 s, 0.5 s and 1 s.

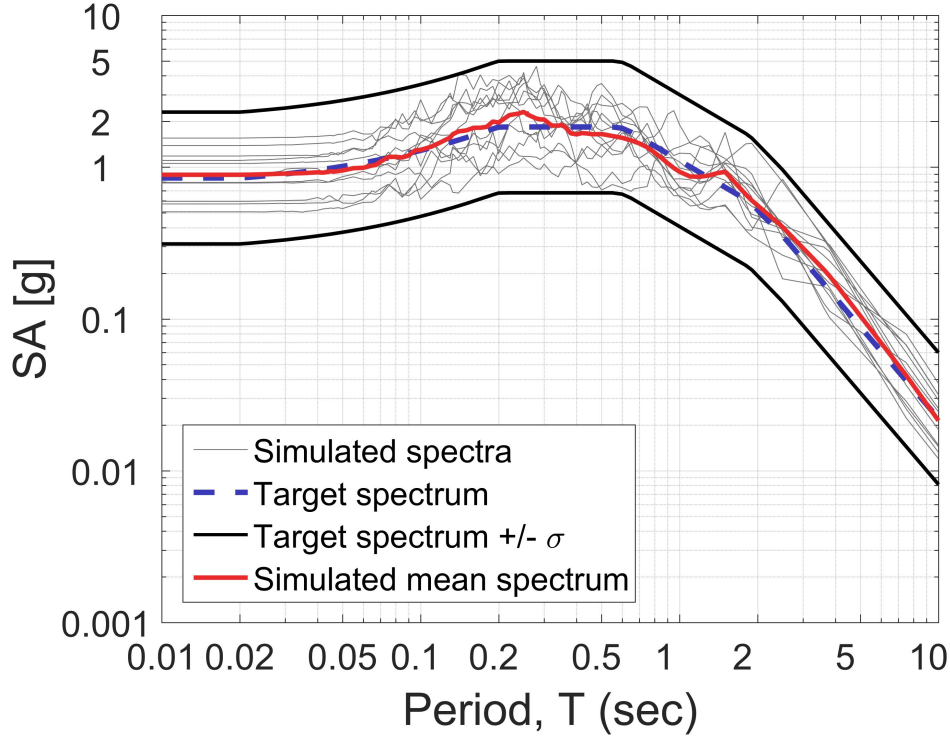


Figure 2.10: Suite of stochastic ground motions matching Eurocode 8 design spectrum. κ filter is set to 0.08 s, logarithmic standard deviation σ to 1 .

2.6 Application from a design spectrum

In this section, a brief example of a procedure to obtain a suite of stochastic ground motions spectrum compatible with a design spectrum is presented. The example proposed is computed from the Eurocode 8 design spectrum with ground acceleration a_g equal to 0.8 g and soil category C . FAS model parameters and κ are generated by the procedure described previously. A set of stochastic ground motions (in our example 50) is computed. The definition of an user-defined threshold provides the remotion of all simulated spectra that show an excessive dispersion around the target spectrum. In figure 2.10 are plotted 35 simulated spectra from a set of 50 realizations. The average spectrum (red line) obtained from this suite fulfills the required spectrum compatibility by Eurocode 8.

2.7 Conclusions

A method for obtain a Fourier amplitude spectrum model (FAS) from a response spectrum has been developed. Nonlinear regression provides a FAS model from set of white-noise samples adjusted to match the response spectrum. The application of kappa filter provides the matching in the short periods part of the target response spectrum.

Tests on suite of simulated spectra generated from NGA-West2 ground motions prediction equation showed excellent matching regarding mean and dispersion values. Further tests on CMSs showed this methodology can be applied successfully from them.

A recent model of inter-frequency correlation in the FAS was applied in our tests. They showed consistency with well-known model for spectral acceleration correlation in terms of shape. However, a general overestimation was obtained, especially in range of short periods.

Simplicity and small time demand are the main virtues of this methodology. Nevertheless, the methodology is constructed on physic assumptions and relies on target response spectrum as basic input, which can be defined in several site conditions (e.g. fault parameters, regional characterization), providing more functionality to the model.

An application for selection of ground motions matching a design spectrum has been presented. After the generation of a large set of time-histories, all simulations out of user-defined boundaries are removed. This procedure allows to obtain suite of stochastic ground motions spectrum-compatible with an assigned dispersion around the design spectrum.

Chapter 3

Analysis of phase derivatives distribution and application for stochastic ground motions

3.1 Abstract

Phase derivatives distributions of the PEER NGA-West1 database are estimated and the relationship between the distribution dispersion and seismological parameters are evaluated. The shape parameter of logistic distribution is proposed as an appropriate measure of dispersion of the phase derivative. First, the relation between the shape parameter and the significant duration (5-75% Arias intensity) is used to check database for outliers. Second, an empirical relation relating shape parameter with moment magnitude, rupture distance, soil category and rupture directivity is developed using non-linear regression. Three applications of the phase derivative models for stochastic ground motion models with a given Fourier amplitude spectrum are proposed: (i) random logistic-distributed phase angles, (ii) calibration of an exponential time window consistent with the phase derivatives shape parameter, and (iii) generation of a near fault pulses using a modified phase difference distribution.

3.2 Introduction

Despite several models were efficiently built to recreate the Fourier Amplitudes of earthquake ground motions (Boore, 2003), nowadays modeling Fourier phase angles is a difficult task and still purpose of studies. Ohsaki (1979) defines, for the first time, phase differences and their importance in signal non-stationarity. They are computed as follow:

$$\Delta\Phi = \Phi_{i+1} - \Phi_i; i = 0, 1, \dots, N/2 - 1 \quad (3.1)$$

Phase differences are usually represented by histogram in a range between between 0 and 2π . They show a 'normal-like' probability distribution, which has the feature to recreate the ground motion shape: typically the mean represents the position of peak in time-domain and the standard deviation "the broadness" around the peak. T. Yokoyama, Watabe (1988) built a model to define each phase difference in a range of 36 values, according to magnitude, fault distance and soil category. Thráinsson, Kiremidjian (2002) divided phase angles in three categories, small, intermediate and large related to Fourier amplitude. They define mean and standard deviation prediction equations from magnitude, distance from the site to source and soil category for each Fourier amplitude category. However, the goodness of these models is affected by the signal length of each record; in other words, different phase differences distributions are obtained from the same record by changing the signal length. For this reason, in this study the authors propose to normalize phase differences by signal length, namely to build a model based on phase derivatives. The presence of fat tails in phase derivatives suggested the application of distribution with kurtosis higher than the normal distribution (i.e. leptokurtic distributions) such as the Logistic distribution. The shape parameter of logistic distribution is chosen as a dispersion measure of phase derivatives. A prediction equation of the shape parameter is defined according to magnitude, rupture distance, soil category and directivity is defined. Eventually, three applications for accelerograms simulation are proposed.

3.3 Phase angles processing and probability density functions

The research was carried out in a database of 3551 recorded ground motions coming from the NGA (B. Chiou, Silva, 2008). Only records with rupture distance lower than *50 km* were processed. Equation 3.2 defines phase derivatives computed for each record.

$$\dot{\Phi} = \frac{\Delta\Phi}{\Delta f} \quad (3.2)$$

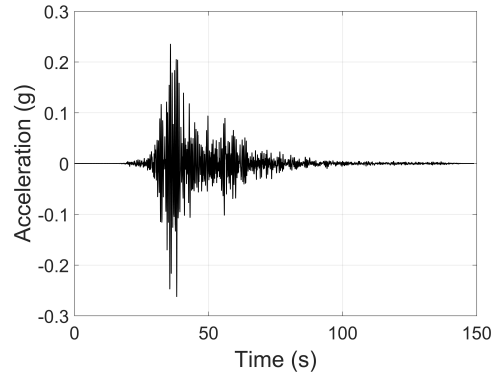
The normalization by signal length provides that dissimilarities between each distribution are exclusively affected by seismological parameters and not by computation process. Each phase derivatives distribution was processed by considering phase angles within a range of frequency between *1 Hz* and *10 Hz*. Furthermore, a filter removed every phase derivative with a value of exceedance probability below 30% of the empirical cumulative distribution. This process provided the removal of noise.

A simple visual check of phase derivatives distributions highlighted that they typically show distribution with fat tails. Such behavior is confirmed by fitting a normal distribution and comparing it with the histogram of probability density function. Thus, the employment of a leptokurtic distribution is proposed; for this purpose, the logistic distribution is selected. Logistic distribution is a "normal-shaped" distribution with higher kurtosis defined by means of mean (μ) and a scale parameter (σ); the probability density function is given by:

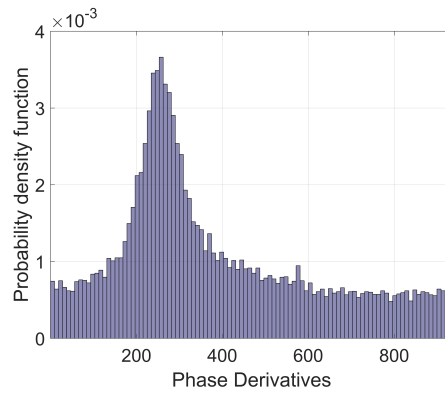
$$f(x; \mu, \sigma) = \frac{e^{-\frac{x-\mu}{\sigma}}}{\sigma(1 + e^{-\frac{x-\mu}{\sigma}})^2} \quad (3.3)$$

Figure 3.1 shows processed phase derivatives of ChiChi event along with normal and logistic distributions; this is a clear example of the better goodness of fit obtained by logistic distribution.

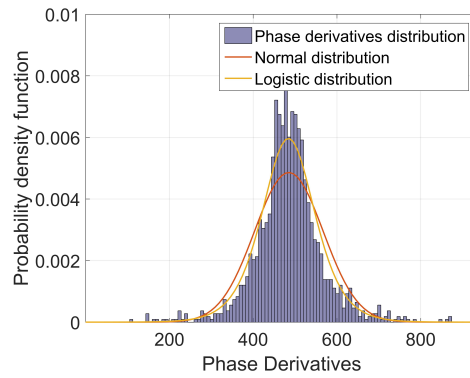
Aim of following regression analyses is to obtain a model for predict σ . In this context, we consider μ as a fixed parameter used to position the distribution along the signal length; thus, it is not a purpose of study. σ is derived by maximum likelihood estimation.



(a) Chichi earthquake record.



(b) Unprocessed phase derivatives.



(c) Centered and filtered phase derivatives.

Figure 3.1: ChiChi earthquake record and its phase derivatives.

3.4 Model definition

Analysis involves the definition of an equation relating the significant duration SD (time between 5% and 75% of Arias intensity) and phase derivatives shape parameter. By means of equation 3.4, a model based on well-known relations (eq. 3.5) between duration and seismological parameters is created.

$$\log(\sigma/\pi) = \alpha_1 + \alpha_2 \log(SD) \quad (3.4)$$

$$SD = D_M + D_{Rrup} + D_{Vs30} + D_{Dir} \quad (3.5)$$

In detail, theoretical seismic source models (Boore, 2003) defines that magnitude influences duration through corner frequency (f_c) ratio (eq. 3.6). Equation 3.7 shows typical form of equations describing corner frequency with event magnitude. Replacing it in equation 3.6 we find the magnitude contribution 3.8.

$$D_M = \frac{1}{f_c} \quad (3.6)$$

$$f_c = 10^{\alpha - \beta M} \quad (3.7)$$

$$D_M = 10^{\beta M} \quad (3.8)$$

Atkinson, Boore (1995) propose a linear proportion between rupture distance and duration:

$$D_{Rrup} = \beta R_{rup} \quad (3.9)$$

Near-surface shear-wave velocity logarithm is set as soil category contribution.

$$D_{Vs30} = \beta \log(V_{s30}) \quad (3.10)$$

The directivity effect on phase derivatives is examined. Two parameters are proposed: (i) ratio between hypocentral and rupture distance and (ii) difference between hypocentral and rupture distance.

$$D_{Dir} = \beta \frac{R_{hyp}}{R_{rup}} \quad (3.11)$$

$$D_{Dir} = \beta (R_{hyp} - R_{rup}) \quad (3.12)$$

Regression analysis is conducted in three stages:

1. Linear regression aiming to find α_1 and α_2 in equation 3.4.

2. Non-linear regression aiming to find β_1 , β_2 , β_3 and β_4 in equation 3.13.

$$\log(\sigma/\pi) = \alpha_1 + \alpha_2 \log[\beta_1 + 10^{\beta_2 M} + \beta_3 R_{rup} + \beta_4 \log(V_{s30})] \quad (3.13)$$

3. Non-linear regression aiming to find γ_1 and γ_2 with all parameters fixed by previous regressions for the two directivity parameters proposed in equations 3.11 and 3.12.

$$\log(\sigma/\pi) = \alpha_1 + \alpha_2 \log[\beta_1 + 10^{\beta_2 M} + \beta_3 R_{rup} + \beta_4 \log(V_{s30}) + (\gamma_1 + \gamma_2 D_{Dir})] \quad (3.14)$$

3.5 Regression analysis

3.5.1 First stage

Linear regression is carried out to find α_1 and α_2 in equation 3.4. Significant duration values are acquired by the PEER report 2013/03 (D. Ancheta, 2013). A scatter plot (fig. 3.2a) shows pairs SD - σ/π along with the line obtained by regression. A comparison with equivalence line highlights smaller steepness for regression line; namely σ tends to less increase than significant duration.

Residuals distribution shows a right-skewed behavior (fig. 3.3a); a limit of 0.3 in residuals allows the exclusion of a relevant part of outliers (see fig. 3.2b). These outliers show excessively broad or narrow phase derivatives dispersion, not in accordance with SD variation; they can be identified as (i) time-histories containing two earthquakes (aftershock) or (ii) time-histories with abnormal presence of surface waves due to basin effect (see fig. 3.4 for an example). Quantile-quantile plot in figure 3.3b shows a remarkable improvement after the exclusion of such records.

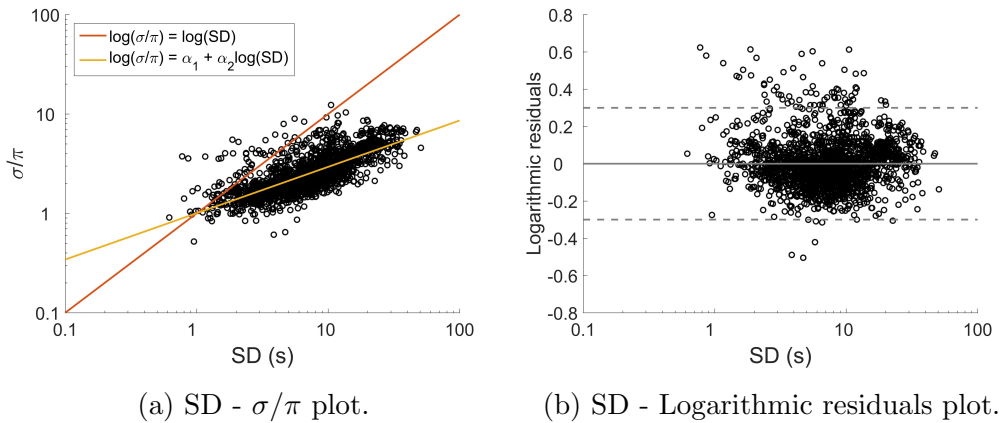


Figure 3.2: First stage regression plots.

3.5.2 Second stage

Non-linear regression is conducted to define β_1 , β_2 , β_3 and β_4 in equation 3.13. Table 3.1 reports parameters obtained by first and second stages. Ac-

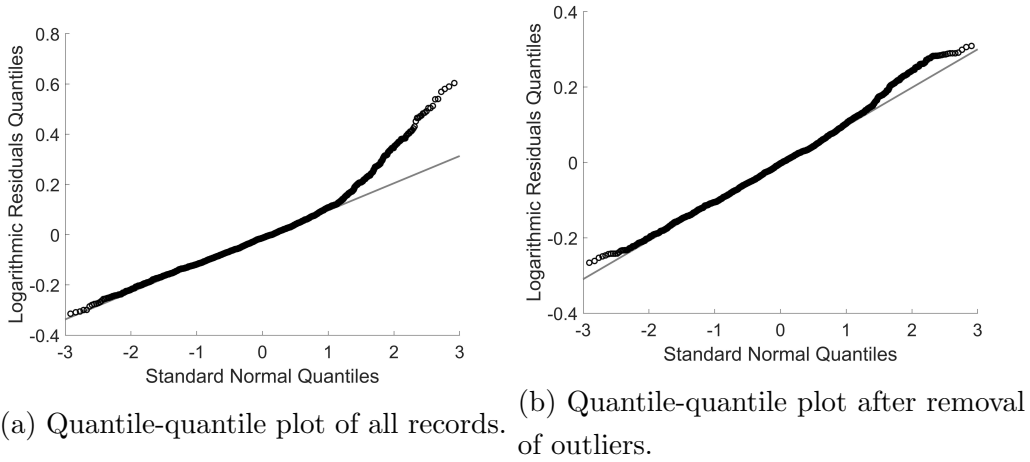


Figure 3.3: First stage residuals quantile-quantile plot.

Table 3.1: First and second stage parameters.

α_1	0.0019
α_2	0.4664
β_1	-6.1722
β_2	0.1707
β_3	0.1360
β_4	-1.2739

According to Boore (2003); Atkinson, Boore (1995), we expected values of β_2 and β_3 around, respectively, 0.5 and 0.05. However, the regression led to a smaller value than expected β_2 and a larger value than expected β_3 . Several attempts were carried out by set a fixed value of β_2 or β_3 , nevertheless unacceptable goodness of fitting reduction was obtained in every case. Table 3.2 reports the correlation matrix of four parameters; the correlation between β_2 and β_3 is -0.20 , excluding a trade-off between the two parameters. Figure 3.5 shows logarithmic residuals versus magnitude, rupture distance and soil category. Overall, no trend is detected from the comparison between logarithmic residuals and each parameter. Furthermore, quantile-theoretical quantile plot (fig. 3.6) shows that we can reasonably defines residuals normally distributed within plus and minus 1 standard deviation bounds.

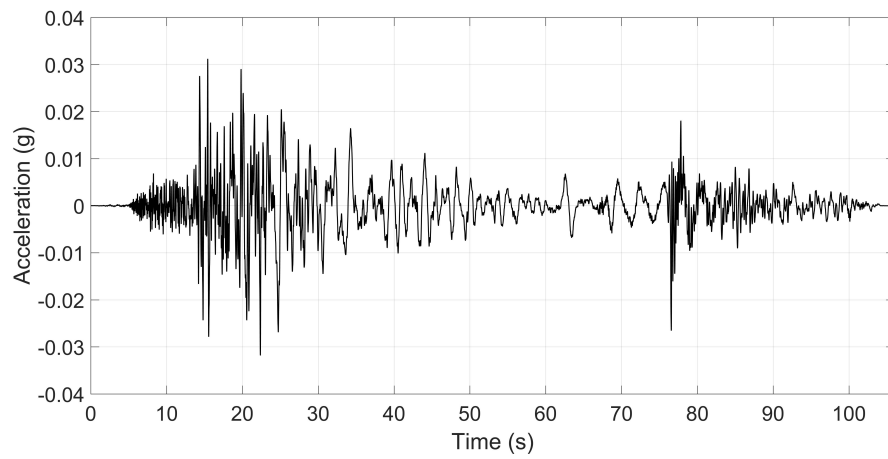


Figure 3.4: ChiChi earthquake record. This is an example of record removed from regression analysis.

Table 3.2: Second stage correlation matrix.

$$\begin{bmatrix} 1 & -0.36 & -0.24 & -0.97 \\ -0.36 & 1 & -0.20 & 0.15 \\ -0.24 & -0.20 & 1 & 0.23 \\ -0.97 & 0.15 & 0.23 & 1 \end{bmatrix}$$

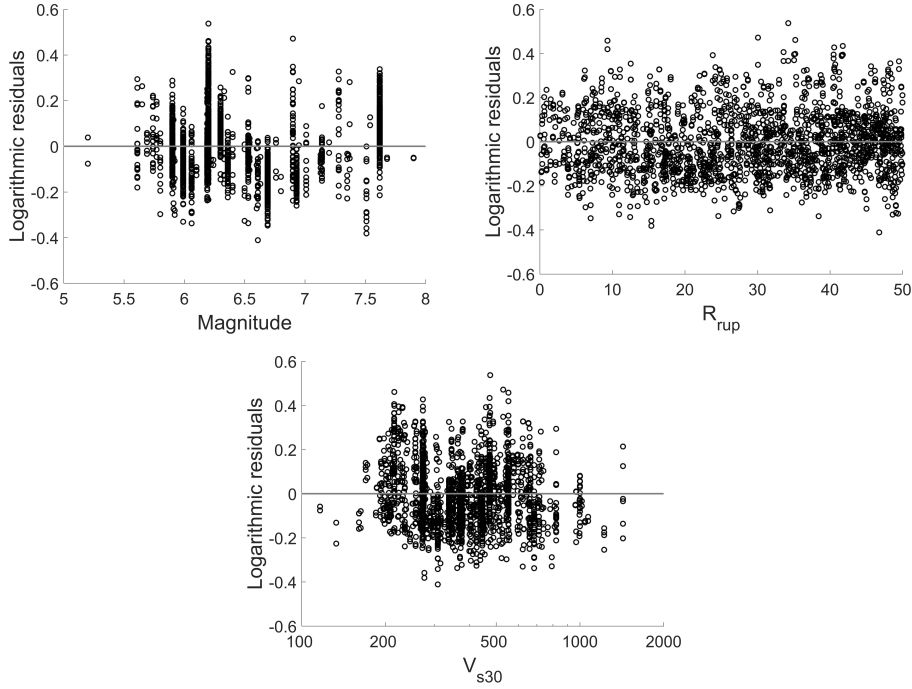


Figure 3.5: Logarithmic residuals versus magnitude, rupture distance and soil category.

3.5.3 Third stage

In the third stage, the effect of directivity is taken into account. Non-linear regression analysis is performed with parameters obtained by the previous stages. Table 3.3 shows γ_1 and γ_2 from equation 3.14. Results from both analyses define a very low dependency of phase derivatives on directivity effect explicated by ratio or difference between hypocentral and rupture distance. Moreover, the low correlation reported in table 3.4 validates the results obtained by the directivity expressed by the ratio; conversely, high correlation of difference parameter discredits its goodness of fit. Quantile-quantile plot is not reported owing to the negligible observed improvement. It is necessary to be cautious about this result, because the directivity should be an important effect on phase derivatives. For this reason, a reflection about the presence of directivity effect in phase derivatives distribution is proposed within the conclusions.

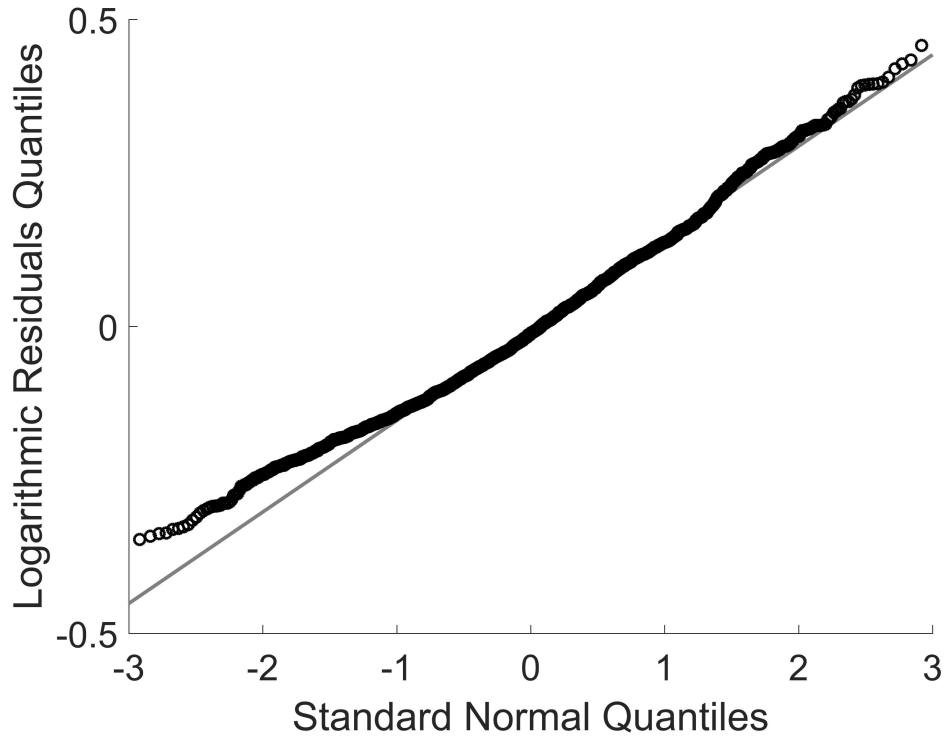


Figure 3.6: Second stage residuals quantile-quantile plot.

Table 3.3: Parameters obtained by third stage regression.

	R_{hyp}/R_{rup}	$R_{hyp} - R_{rup}$
γ_1	0.0055	0.0748
γ_2	-0.0020	-0.0107

Table 3.4: Third stage correlation matrix.

(R_{hyp}/R_{rup})	$(R_{hyp} - R_{rup})$
$\begin{bmatrix} 1 & -0.21 \\ -0.21 & 1 \end{bmatrix}$	$\begin{bmatrix} 1 & -0.72 \\ -0.72 & 1 \end{bmatrix}$

3.6 Applications

Prediction of phase derivatives dispersion can be used in stochastic ground motion generation. We consider that a Fourier amplitude spectrum (FAS) has already been computed and the application of phase angles provides the non-stationarity. Two methods are proposed for obtain phase angles to combine with FAS. Moreover, a method for create near fault pulses for stochastic ground motions is proposed. The three applications are subject of the next three subsections.

3.6.1 Random logistic-distributed phase derivatives

1. Estimation of σ by means of equation 3.13.
2. Generation of Random logistic-distributed phase derivatives (mean value set to π/df for centered peak).
3. Multiplication by df in order to obtain phase differences.
4. Phase angles generation from phase differences (first phase angle can be random or arbitrary set).
5. Apply obtained phase angles to FAS model and inverse Fourier transform.

An example of stochastic ground motions obtained by this procedure is plotted in fig. 3.7 along with its phase differences.

Arias intensity of a suite of real records and another suite of stochastic ground motions suites is plotted in Figure 3.8. Records are selected from NGA-West2 database by search parameters: $6.5 < M < 7.5$, $1 < R_{rup} < 20$ km , $760 < V_{s30} < 2000$ m/s; suite of stochastic ground motions is generated from an uniformly sorted selection of the same parameters by the methodology proposed in chapter 2. Stochastic ground motions arias intensity matches remarkably the real records behavior within a range of most interest (0% - 75%). Such concept is confirmed by the mean value comparison, which shows mismatching exclusively in the upper tail.

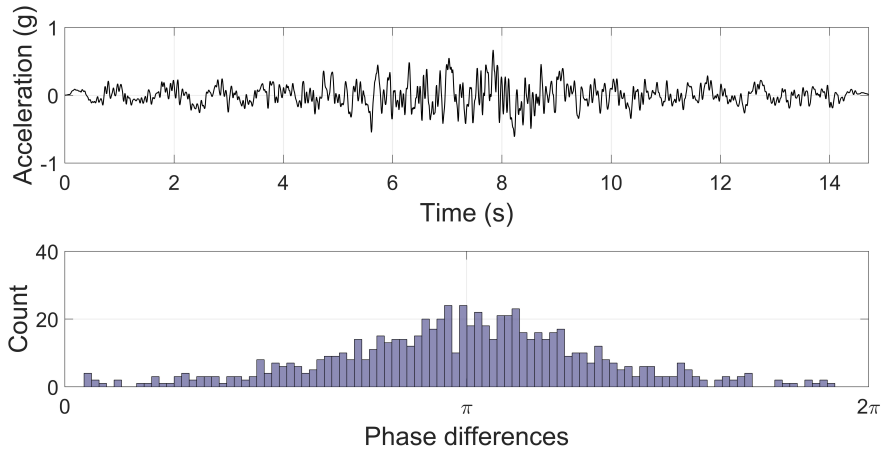


Figure 3.7: Stochastic ground motion generated by random logistic-distributed phase derivatives.

However, a comparison in terms of range (i.e. the difference between maximum and minimum value) shows a general underestimation; which implies that a part of phase derivatives variability is not taken into account in the model proposed.

3.6.2 Exponential window calibration

A common procedure is windowing a white-noise by an exponential function (Saragoni, Hart, 1973), Fourier transforming, computing phase angles and applying them to FAS model. An analysis about the relationship between signal total duration and σ of phase derivatives obtained by this procedure was carried out. In detail, several white-noise samples of different total duration were generated and windowed by an exponential window with parameter $\epsilon = 0.2, \eta = 0.05$; therefore phase derivatives shape parameter was computed for each sample. Figure 3.9 shows regression lines from the white noise and the equivalent procedure applied to stochastic ground motions. In both cases, we considered phase derivatives within 1 Hz and 10 Hz . Two regression lines are reasonably equivalent, validating the application of such relationship to find the total duration of a windowed signal, which phase derivatives distribution shows a desired shape parameter value. Definitely, the procedure

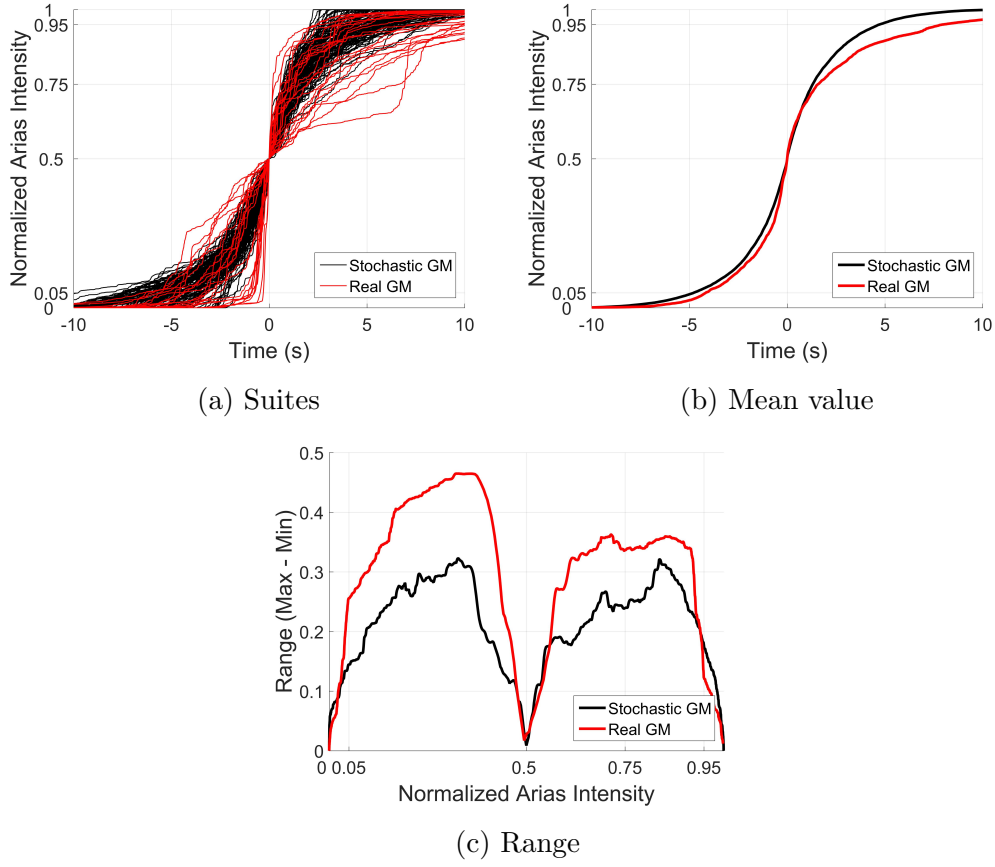


Figure 3.8: Comparison between a suite of real ground motions and stochastic ground motions in terms of Arias intensity. Time zero is set at 50% of Arias intensity.

can be summarized as follow:

1. Estimation of σ by means of equation 3.13.
2. Find the total duration (TD) for the white-noise.

$$TD = -4.21 + 2.156\sigma \quad (3.15)$$

3. Generate a white noise with duration TD.
4. Apply the exponential windows with parameter $\epsilon = 0.2, \eta = 0.05$.
5. Fourier transform and phase angles computation.

6. Apply obtained phase angles to FAS model and inverse Fourier transform.

Likewise the first procedure, this process provides a final result with phase derivatives distribution compatible with the imposed shape parameter. Nevertheless, the exponential window shows asymmetric shape typical of earthquakes that is not reproducible with phase derivatives logistic-distributed.

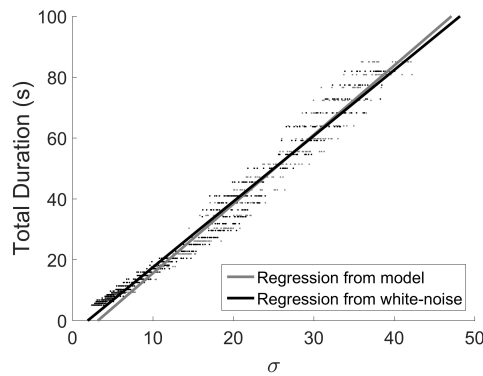


Figure 3.9: Regression lines expressing the relationship between signal total duration and phase derivatives shape parameters.

3.6.3 Pulse creation

Fixing the values of phase derivatives within frequency range of $0-1$ Hz in the center of distribution allows the creation of a velocity pulse in simulated accelerograms. According to the chosen procedure, it is necessary to change phase derivatives for: π/df (centered random logistic-distributed phase derivatives) or $0.4\pi/df$ (exponential window with $\epsilon = 0.2$). Figure 3.10 shows an example of stochastic ground motion generated by exponential window and modification of phase angles below 1 Hz.

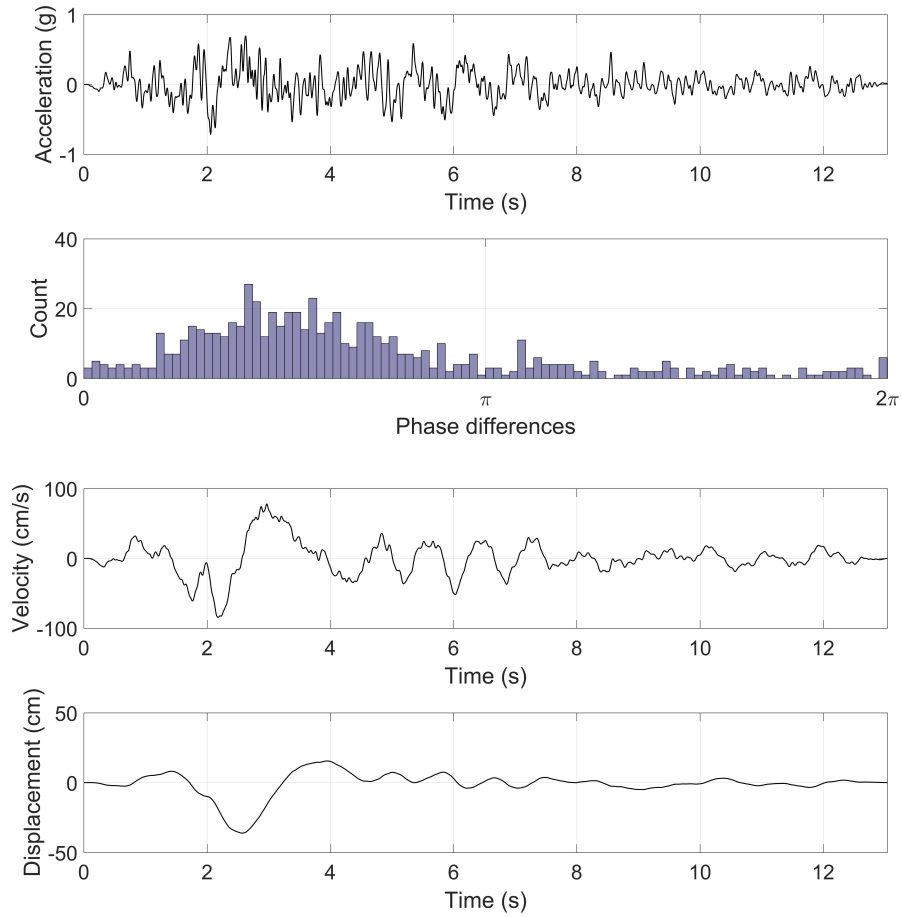


Figure 3.10: Acceleration, phase differences, velocity and displacement of a stochastic ground motion generated by exponential window phase angles. The record contains a velocity pulse created by centering phase differences below 1 Hz .

3.7 Conclusions

A study about phase derivatives distribution through the NGA-West1 database has been proposed. The presence of fat tail in distributions suggested an application of leptokurtic distribution. A remarkable improvement in the goodness of fit process has been obtained by implementing logistic distribution.

Three stages regression analysis has been carried out. First stage defined a prediction equation between logistic distribution shape parameter and significant duration. Shape parameters are computed by means of maximum likelihood estimation after a process of noise removing in each record. Second stage defined the relationship between phase derivatives dispersion and magnitude, rupture distance, soil category. Output parameters showed that phase derivatives dispersion increases less than expected with magnitude and is more affected by the rupture distance contribution. Third stage demonstrated a very low dependency to directivity effect explicated as ratio or difference between hypocentral and rupture distance. Although this result seem to deny dependency of phase derivatives on directivity, the author's opinion is that the directivity effect is inside the overall distribution. In particular, we suggest that two distributions, corresponding two separate frequency ranges, in combination recreates the distribution studied in this paper. The two distributions should have different position and broadness; the distance between the two mean values should reproduce a directivity effect estimation.

Phase derivatives dispersion prediction equation can be used for generation of stochastic ground motions; three applications are proposed. First application is the imposition of phase angles from random logistic-distributed phase derivatives. Arias intensity function of stochastic ground motions obtained by this procedure and real records has been compared. In particular, two suites (selected by parameters $6.5 < M < 7.5$, $1 < R_{rup} < 20$ km , $760 < V_{s30} < 2000$ m/s) showed notable matching in terms of shape. Range comparison suggested that further studies are necessary to take into account the entire variability of phase derivatives distribution. As previously declared, the frequency dependency of distributions is an important feature to

consider in phase derivatives variability in future works. Second application regards the calibration of exponential window for generation of phase angles by windowing a white-noise. The selection of a proper signal duration provides the desired phase derivatives dispersion; an equation is proposed for this aim. The equation has been successfully tested with a methodology of stochastic ground motion generation. Third application allows the creation of velocity pulse by modifying phase derivatives for frequency below 1 Hz ; the effect is obtained by centering phase derivatives in the distribution.

Chapter 4

Conditional scenario spectra generation through simulated spectra

4.1 Abstract

A stochastic ground motions generation methodology with realistic variability and inter-frequency correlation of the FAS and phase derivatives is used to develop suite of time histories for the conditional scenario spectra (CSS). The CSS are a set of response spectra with assigned rates of occurrence that reproduce the hazard over a wide range of hazard levels and spectral periods at one site. The CSS provide an estimate of the seismic history for a site in terms of the time histories likely to be experienced at the site. These time histories and their rates are then used to estimate the hazard curve for engineering demand parameters. The method used for generate stochastic ground motions is based on matching target response spectra which is the main set of CSS. The main advantages of this application are: (i) the small number of time histories (generally less than one hundred) required to reproduce the hazard compared to methods that use recorded time histories, and (ii) the very fast computation.

4.2 Introduction

Selection of ground motions in earthquake design is the first step for non-linear response study. The typical routine is based on obtain values of magnitude and distance based from site hazard deaggregation and search for records that respects those values within a certain range. Response spectrum matching is taken into account by selecting only records that match a target response spectrum (if available) or by modifying the frequency content. Output of this procedure is a small set of accelerograms, which provides the estimation of the median response of your structural system. A change in the process of selection and a consequent larger set of accelerograms is required to consider the response variability. Incremental Dynamic Analysis (Vamvatsikos, Cornell, 2002) is one of the existing approaches. It consists in selection of a set of ground motions, which are scaled progressively to reconstruct a fragility curve showing variation of an important structural parameter versus a parameter describing record intensity. The assumption of this methodology is that intensity variation is only related to a scaling factor and not to a change in other features (e.g. response spectrum shape, duration). The Conditional Scenario spectra (CSS) is a selection of set of spectra with assigned rate of occurrence, which is able to reproduce site seismic history. CSS adds the intrinsic variability of earthquakes by selecting a wider range of spectra, which shape is consistent with the hazard level represented. Arteta (2017) presents a description of CSS methodology and offers an example of its application. In this chapter, a detailed procedure of CSS computation by means of stochastic ground motions is presented. The aim of this study is to highlight the pros of a such application, and propose a standard procedure to obtain the CSS from a set of Uniform hazard spectra by means of stochastic ground motions.

4.3 Conditional Scenario Spectra definition

A typical set of CSS is plotted in fig. 4.8a. Each spectrum has an assigned rate of occurrence, which is represented in fig. 4.8b. The hazard can be estimated from the CSS by a generic test value of spectral acceleration. The usual aim of a case study is to reproduce a set of uniform hazard spectra, obtained by probabilistic seismic hazard analysis (PSHA). Therefore, an estimation of hazard from CSS is represented in equation 4.1

$$\nu(SA(T) > SA_{UHS}(T)) = \sum_{i=1}^N Rate_i * H(SA_i(T) - SA_{UHS}(T)) \quad (4.1)$$

The hazard ν of exceeding a spectral value SA greater than SA_{UHS} (uniform hazard spectrum value) is provided by sum of rates of occurrence $Rate_i$ of scenario spectra which show a spectral value SA_i greater than SA_{UHS} . The aforementioned condition is mathematically represented by the heaviside function $H(SA_i(T) - SA_{UHS}(T))$, expressed in equation 4.2.

$$H(SA_i(T) - SA_{UHS}(T)) = \begin{cases} 1 & SA_i(T) \geq SA_{UHS}(T) \\ 0 & SA_i(T) < SA_{UHS}(T) \end{cases} \quad (4.2)$$

The rates of occurrence are calibrated to provide an hazard ν , which matches PSHA hazard in range of all structural periods (see fig. 4.7). The potentiality of CSS lies in the usage of rates of occurrence to build risk curves of engineering demand parameters (EDP). Each ground motion can be run through a structure model to obtain an EDP (e.g. interstory drift) and construct risk curve by equation 4.3.

$$\nu(EDP > d) = \sum_{i=1}^N Rate_i * H(EDP - d) \quad (4.3)$$

Further informations about risk curves estimation are provided in Arteta (2017). The next section details the methodology used to generate a set of stochastic ground motions consistent with seismological history of a site and the calibration of rates of occurrence to match the Uniform hazard spectra from PSHA.

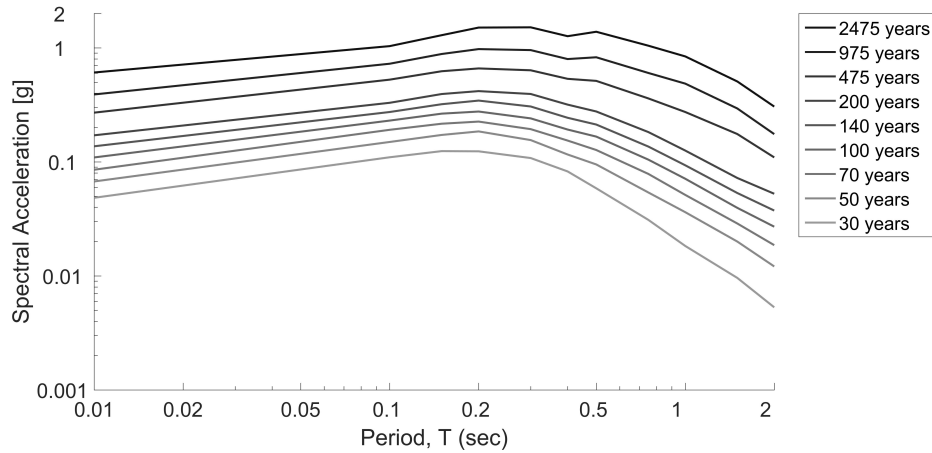


Figure 4.1: Uniform hazard spectra in Francofonte, Sicily.

4.4 Procedure of CSS creation

A real case study is proposed as example to describe the process of CSS creation. Francofonte, a Sicilian location is the chosen site. Uniform hazard spectra (fig. 4.1) as well as the mean values of magnitude and distance (tab.4.1) are obtained from Italian interactive seismic hazard map. Next subsections describes in detail the procedure divided in three steps:

- GMPEs generation.
- Scenario spectra selection.
- Rates of occurrence calibration.

4.4.1 GMPEs generation

The procedure involves the computation of one GMPE for each hazard level. GMPEs calibration depends on site condition; in particular, deaggregation provides values of magnitude and rupture distance (see table 4.1). In the example proposed, the geometric mean [0.22ASK 0.22BSSA 0.22CB 0.22CY 0.12IM] of NGA-West2 equations (N. A. Abrahamson, Kamai, 2014; D. M. Boore, Atkinson, 2014; Campbell, Bozorgnia, 2014; Chiou, Youngs,

Table 4.1: Mean values of magnitude and distance for different return periods in Francofonte, Sicily.

Return Period (yrs)	2475	975	475	200	140	100	70	50	30
M	6.58	6.31	6.11	5.87	5.77	5.67	5.56	5.47	5.32
R	6.03	7.83	9.53	11.9	13.22	14.7	16.8	19.4	25.2

2014; Idriss, 2014) is developed. The other parameters used for GMPEs calibration are chosen by considering fault conditions for the case study.

This step provides a set of GMPEs consistent with every hazard level (see fig. 4.2).

4.4.2 Scenario spectra selection

Suites of stochastic ground motions are generated by means of the methodology described in chapter 2, which provides a Fourier amplitude spectrum model corresponding to each GMPE. The application of phase angles computed by prediction equation of phase derivatives dispersion proposed in chapter 3 provides the non-stationarity to each time-history. Input parameters for phase derivatives prediction are chosen according to the hazard level. The following list describes the procedure of scenario spectra selection:

1. Generation of 100 time-histories for each GMPE by the aforementioned procedure. Every time-history exceeding the mean value ± 3.5 times the standard deviation is removed. Figure 4.3 shows all set of candidate scenario spectra computed for each hazard level.
2. Arbitrary selection of a number of scenario spectra per hazard level N_S (typical between 10 and 20). The total number of scenario spectra N_{tot} is:

$$N_{tot} = N_S * N_{HL} \quad (4.4)$$

Where N_{HL} is the number of hazard levels.

Montecarlo simulation generates a set of selected scenario spectra. Normalized logarithmic residuals $\varepsilon_{SA_{j,i}}$ are computed between each scenario

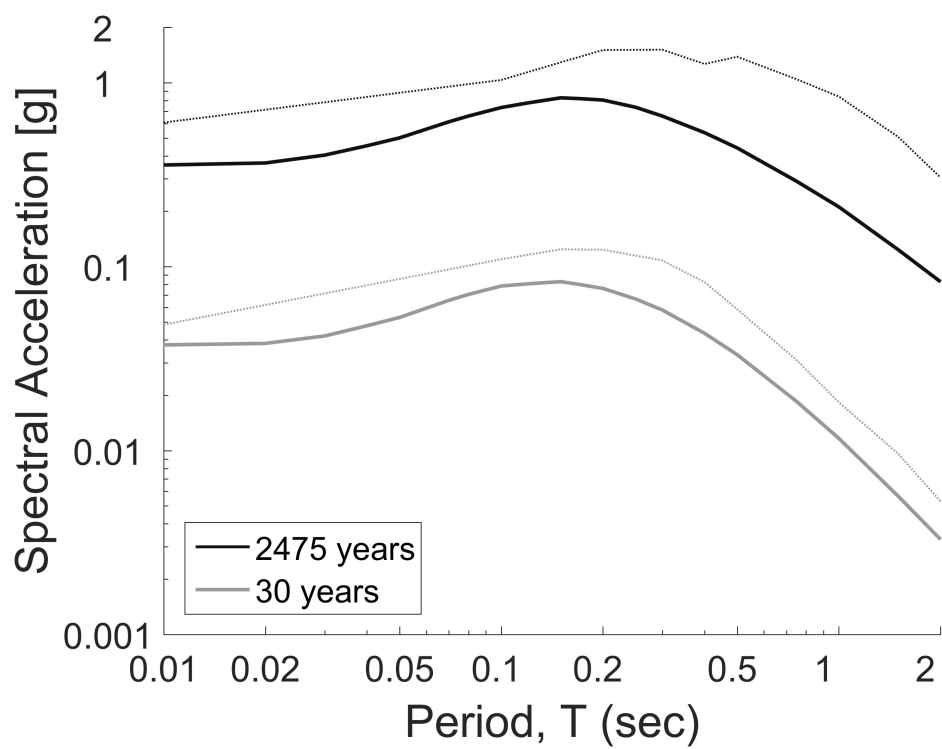


Figure 4.2: Representation of only GMPEs calibrated for the first and last hazard levels along with the Uniform hazard spectra (dotted line).

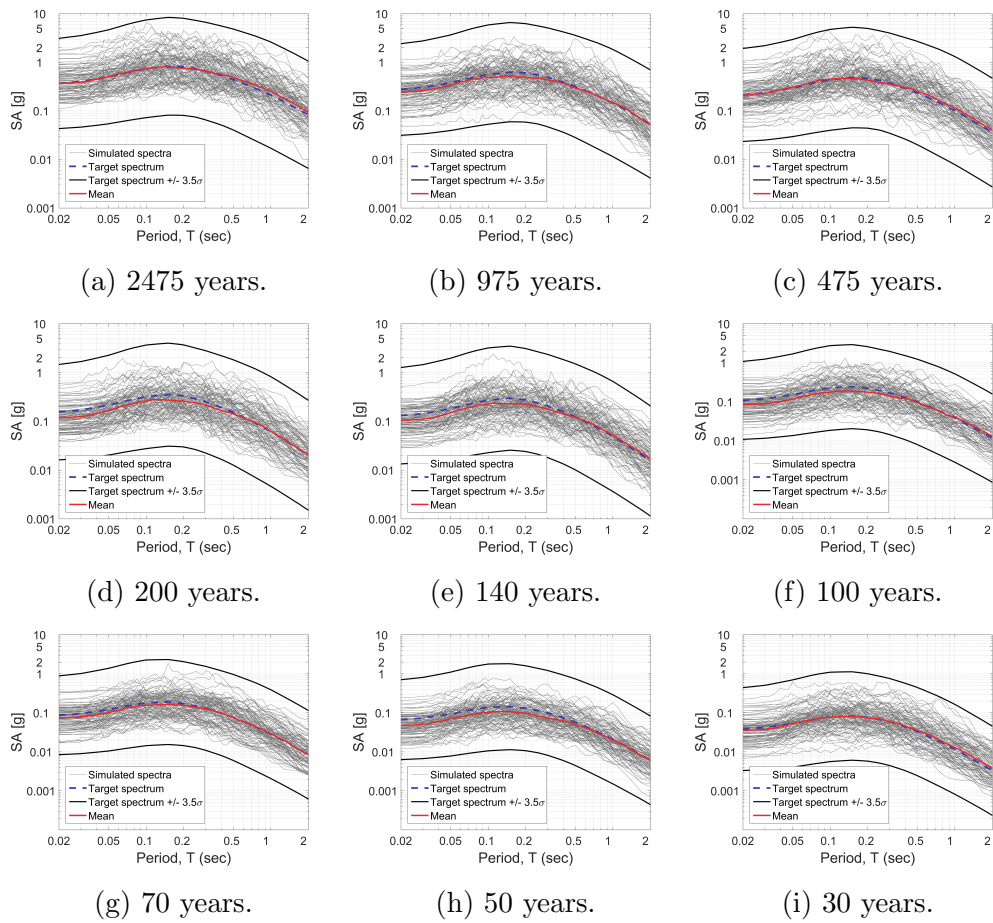


Figure 4.3: Set of candidate scenario spectra computed for each hazard level.

spectra $SA_{j,i}$ and GMPE (SA_{GMPE_j}) corresponding to the hazard level j :

$$\varepsilon_{SA_{j,i}}(T) = \frac{\ln SA_{j,i}(T) - \ln SA_{GMPE_j}(T)}{\sigma_{\ln GMPE_j}} \quad (4.5)$$

This step aims to find a set that optimize the mean value of residuals to zero and the standard deviation to one for each level. Furthermore, the correlation is computed from the all spectra and optimized to match the model proposed by Baker, Jayaram (2008). Figure 4.4 shows the optimization for each level in terms of mean and standard deviation. Figure 4.5 represents the correlation values obtained by all spectra and the model used.

4.4.3 Rates of occurrence calibration

An initial value of rate of occurrence is assigned to the i scenario spectrum corresponding to the j hazard level from the target hazard V_j :

$$Rate_i = \begin{cases} \frac{V_1}{N_S} & 1 < i \leq N_S \\ \frac{V_j - V_{j-1}}{N_S} & N_S < i < N_{tot} \end{cases} \quad (4.6)$$

The levels are counted from the top, the first level correspond to the lowest hazard level. A simple algorithm allows the adjustment of rates of occurrence. It increases or decreases the rate of occurrence of each scenario spectrum aiming to minimize the misfit between the target and hazard computed from CSS. The misfit is defined as the average of squared logarithmic difference for all hazard levels:

$$Misfit = \frac{1}{N_{HL}} \frac{1}{N_T} \sum_{k=1}^{N_T} \sum_{j=1}^{N_{HL}} \log \left(\frac{V_j}{\nu_{j,k}} \right)^2 \quad (4.7)$$

Where $\nu_{j,k}$ is the hazard estimated from CSS for each hazard level j and period k , N_T is the total number of periods. Figure 4.6 shows the comparison between target and estimated hazard for periods 0.1 s and 1 s before and after optimization. Figure 4.7 provides an overview of hazard estimation for all hazard levels and periods. The procedure of calibration includes the exclusion of all spectra with very low contribution. In the example proposed

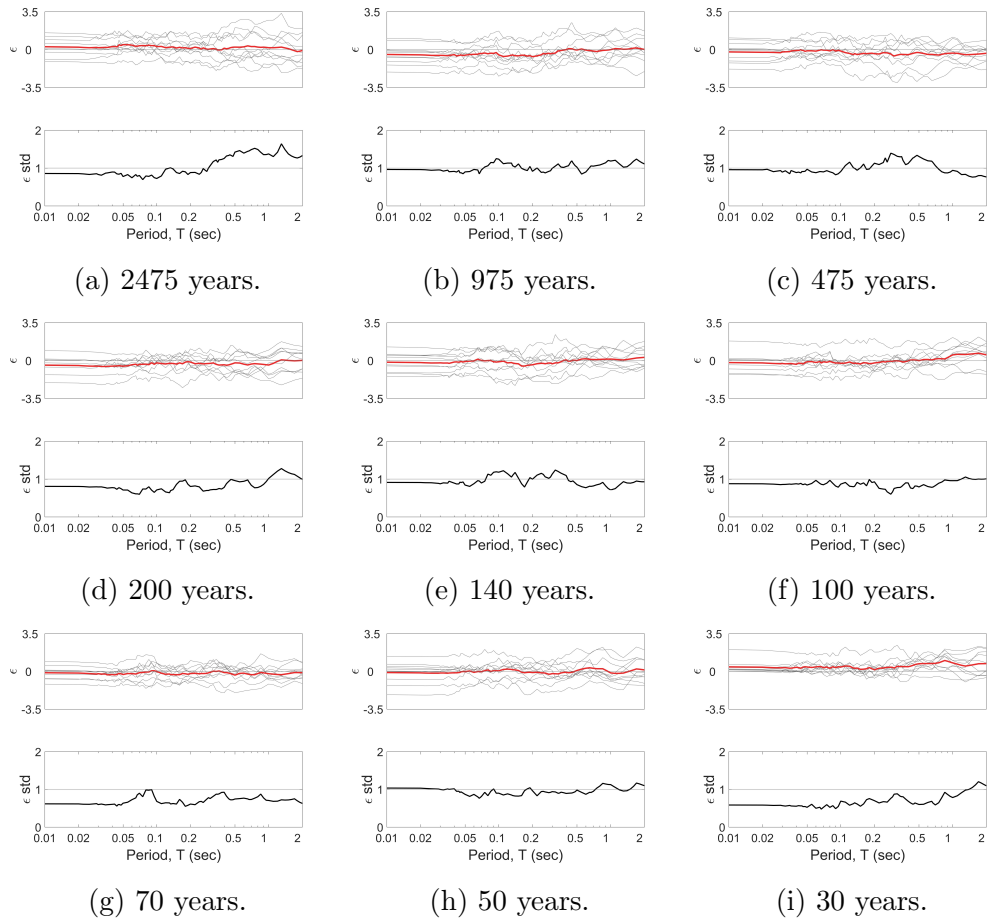


Figure 4.4: Plot of normalized residuals for each hazard level. In first graph, gray lines represent the normalized residuals for each scenario spectrum, red line represent the mean value. In second graph, black line represent the standard deviation of normalized residuals. Montecarlo simulation aims to match red line with 0 and black line with 1 .

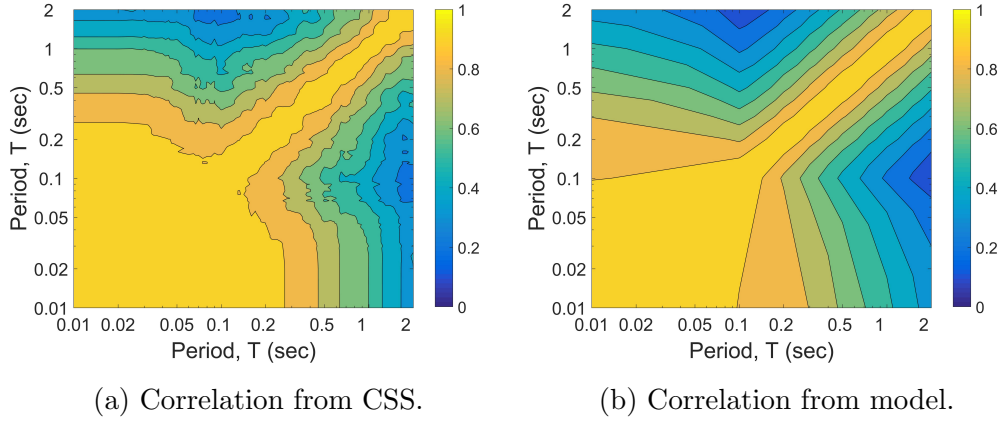


Figure 4.5: Comparison of spectral values correlation. Montecarlo simulation aims to match the correlation represented in the first plot with the second plot.

(see fig. 4.8), 90 scenario spectra are reduced to 84 after the optimization. The usage of weighted average along hazard levels in misfit computation can improve the goodness of fit. Although it privileges high hazard levels by reducing goodness of fit for low hazard levels.

4.4.4 Summary

The entire procedure of CSS generation can be briefly outlined as follow:

- **GMPEs generation** - one set of GMPEs is computed for each hazard level according to site conditions.
- **Scenario spectra selection** - one suite of stochastic ground motions is generated from each GMPE. Only ground motions within a range between the mean target value ± 3.5 times the standard deviation are selected. Monte Carlo simulation is carried out to select a set of scenario spectra able to represent mean, dispersion values of GMS for each hazard level as well as to recreate spectral correlation consistent with a correlation model.
- **Rates of occurrence calibration** - Rates of occurrence are initially estimated as uniform distributed for each level. A process of optimiza-

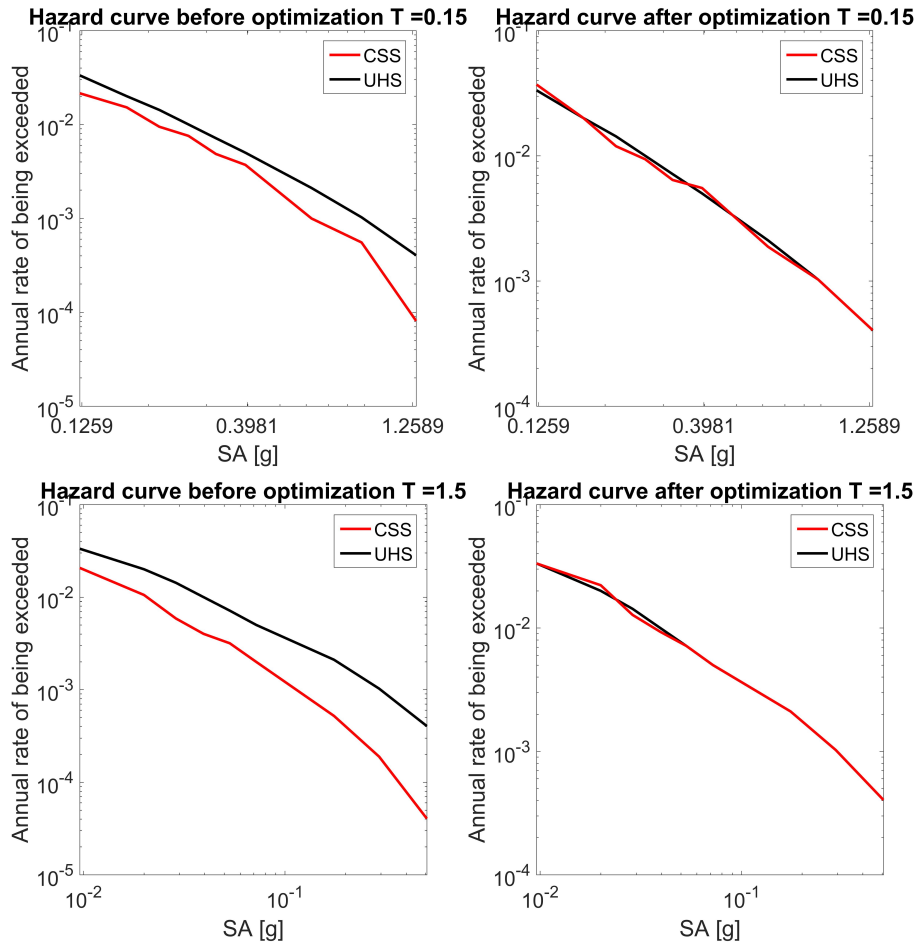


Figure 4.6: Comparison between target and hazard estimated from CSS for periods $0.15 s$ and $1.5 s$ before and after optimization. Application of weighted misfit provides better matching at high levels hazard trading off for a reduction of matching at low hazard levels.

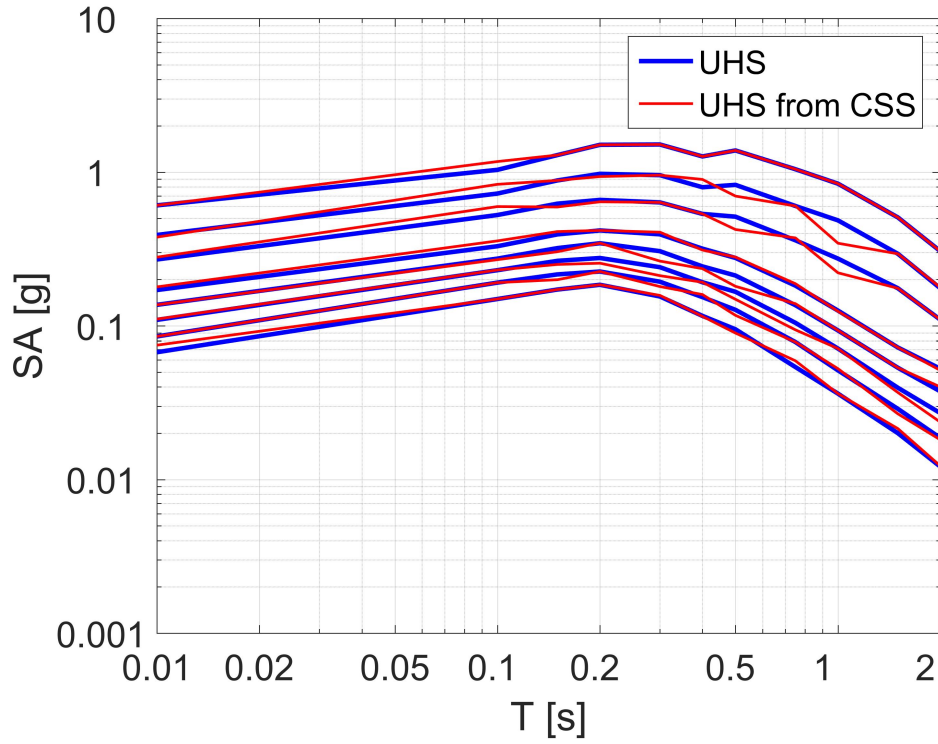
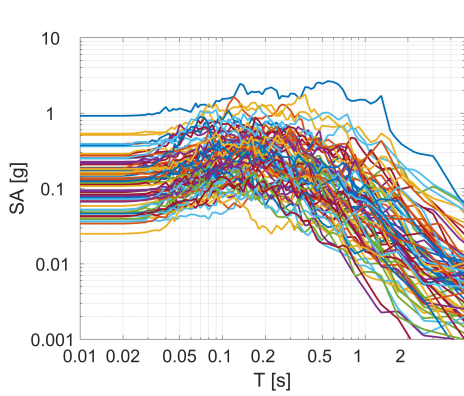
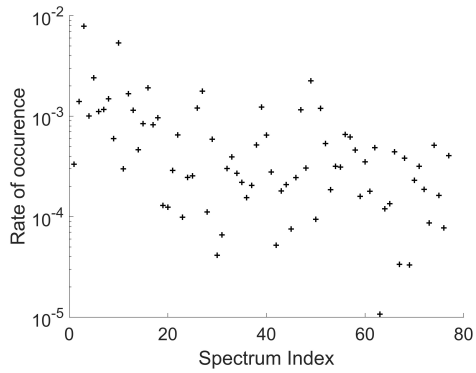


Figure 4.7: Comparison between target UHS and recovered by Conditional scenario spectra UHS.



(a) CSS able to replicate the seismic hazard of example case study.



(b) Rate of occurrence related to each spectrum part of CSS. Spectrum index is sorted from low to high hazard.

Figure 4.8: CSS and rates of occurrence for the case study of Francofonte, Sicily.

tion calibrates rates of occurrence to match the input hazard and exclude every spectrum requiring an excessive changing from the starting value.

4.5 Conclusions

In this chapter a methodology for developing the conditional scenario spectra (CSS) from stochastic ground motions has been proposed. The CSS is a set of response spectra with assigned rates of occurrence, which is able to recreate the seismic hazard of a case study. Rates of occurrence are calibrated to match hazard obtained by probability seismic hazard assessment (PSHA). The application of CSS allows to build risk curves of engineering demand parameters (EDP); in other words, CSS provides an assessment of engineering application behavior in all seismic scenarios through a representative parameter (e.g. interstory drift).

A set of Uniform hazard spectra with assigned hazard and the mean values of magnitude and distance for each level are inputs for CSS generation. The procedure can be divided in three steps.

First, ground motion prediction equations (GMPEs) are developed for each hazard level. Input parameters for GMPEs are mean values of magnitude and distance obtained by deaggregation. In case of GMPEs characterized by further parameters (e.g. soil category, fault mechanism), they can be set according to site condition.

Second, suites of at least 100 stochastic ground motions are generated from each GMPE. The employed methodology is based on Fourier amplitude spectrum model obtained by a target response spectrum (the GMPE in this case); the non-stationarity is achieved by the application of phase derivatives distribution predicted from magnitude, distance and soil category. Monte-carlo simulation random generates small sets of candidate scenario spectra; output of this simulation is a small set of spectra able to represent mean value, dispersion of all GMPEs and show correlation consistent with well-known models.

Third, rates of occurrence are assigned to all scenario spectra. Therefore, the rates are iteratively adjusted to match the input hazard by means of a misfit parameter. At the end of the process, spectra with a low rate of occurrence are removed, because their small contribution to the hazard.

Final result of this procedure is a set of spectra, which amount is less than one hundred. Compared to the method with recorded time histories,

stochastic ground motions allows a remarkable reduction in the total number of spectra. The previous feature as well as the simplicity and speed of the procedure are the main advantages of the proposed methodology. Application of this CSS with engineering structure are expected in future studies.

Chapter 5

Conclusions

This paper proposes a methodology for obtain Fourier amplitude spectrum model (FAS) from a target response spectrum. Response spectra of stochastic ground motions generated from such model matches, on average, the target spectrum. An analysis of phase derivatives distribution of earthquakes records database provides the predictive equation for calibrate a proper distribution to combine with the aforementioned FAS. Non-stationarity of stochastic ground motions is achieved from phase derivatives distribution consistent with the site condition parameters (i.e. magnitude, rupture distance, soil category). All this features contribute to employ stochastic ground motions for create a set of spectra able to represent the seismic history of one site, namely the Conditional Scenario Spectra (CSS). The CSS can be constructed from a set of Uniform Hazard Spectra, by means of ground motion prediction equations (GMPEs) and a proper site characterization. The following sections briefly summarize the important findings of this work, the limitations of this work, and suggested future work related to this paper.

5.1 Fourier amplitude spectrum model

The FAS model is obtained by fitting a generalized source model with a set of adjusted simulated spectra. These spectra are generated consistent with a simple corner frequency model and are adjusted in the frequency content to match the target spectrum. A procedure of non-linear regression provides the

best parameters to shape a FAS model matching the FAS of such adjusted spectra. Attenuation in the high frequency part of the spectrum is obtained by κ filter, calibrated iteratively by visual check. Stochastic ground motions can be obtained from this model by generating random normally-distributed FAS with a mean values which is the FAS model previously described. The usage of a covariance matrix allows to control frequency variance and inter-frequency correlation.

Several tests have been carried out and they showed that suite of stochastic ground motions generated from this procedure are able to match, on average, target spectra such as GMPEs, Conditional mean spectra (CMS) and Design spectra. No scaling or frequency adjustment is included in the procedure. In our tests, a constant variance of 0.8 along with the inter-frequency correlation model proposed in Stafford (2017) allows a remarkable reproduction of NGA-West2 dispersion. The authors tested the FAS model with uncorrelated frequency content (i.e. covariance matrix with null off-diagonal elements) and discovered that the mean spectrum obtained from a suite is, exclusively in the uncorrelated case, dependent on variance values. A constant variance of 0.4 allows the matching in case of uncorrelated frequency content. The potentiality of this methodology lies in the capacity of fully reproduce a target response spectrum. The development of GMPE based on a proper site characterization can be used to generate stochastic ground motions which respect all the feature of earthquakes response spectra.

The only lack of these simulated ground motions is the stationarity of the frequency content. In fact, they are computed without considering that the frequency content varies during a typical earthquake record. Two solutions are available for this aim. The first one is to consider Fourier amplitudes not constant in the time domain. This option includes to define a function describing the Fourier amplitude variation with time, which must be different with the considered frequency. The second option is to apply a phase derivative distribution dependent on the frequency content, as specified in the next section.

5.2 Phase derivatives analysis

The phase angles computed from Fourier transform of an earthquake record contain important information about the time non-stationarity. Distribution of phase derivatives (i.e. phase differences normalized by the signal length) shows a shape consistent with the shape in time domain; in particular, the mean represents the position of peak in time-domain and the standard deviation "the broadness" around the peak. Furthermore, these distributions show a leptokurtic behavior (i.e. higher kurtosis than normal distribution); for this reason, in this paper the application of logistic distribution has been proposed. Such distribution is defined by a mean value and shape parameter.

The analysis proposed in this paper aims to find a predictive equation for the shape parameter from earthquake records (the mean values is ignored in this paper). Three stages regression analysis has been carried out. The first stage establishes an equation relating the significant duration (i.e. 5-75% Arias intensity) with the shape parameter. Second stage creates a relationship between shape parameter and magnitude, rupture distance and soil category by means of the equation found in the first stage. Such equation is based on well-known relationship between significant duration and seismological parameters; for this reason, the shape parameter has been connected with the significant duration. Third stage aims to find dependence of shape parameter with directivity effect. The directivity effect has been tested by two different parameters: ratio and difference between hypocentral and rupture distance.

The first stage allowed to distinguish a group of outliers, identified as records with two earthquakes or record with an abnormal basin effect; all these records have been removed from the analysis. Final parameters showed consistency with typical parameters used with significant duration. However, phase derivatives shows less dependence on magnitude and more dependence on rupture distance than significant duration. Trade-off between the two parameters can be excluded by the low correlation obtained from the correlation matrix. Third stage showed that the directivity can not be considered by one parameter; regression of both parameters showed a very low level of dependence.

Phase derivatives can be used in three different applications for generation of stochastic ground motions. First application is to obtain phase angles from random logistic-distributed phase derivatives. Second application is the calibration of an exponential window from the equation proposed for relate phase derivatives shape parameter with the total duration of the exponential window. This procedure allows to obtain a more realistic shape in the time domain which is consistent in the phase derivatives distribution with the predictive equation. Third application is a modification of phase derivatives below 1 Hz which are centered in the distribution. This modification causes the creation of a near-fault pulse.

Suite of stochastic ground motions has been computed by consideration a all the combination of parameter between $6.5 < M < 7.5$, $1 < R_{rup} < 20\text{ km}$, $760 < V_{s30} < 2000$. Suite of earthquakes records has been selected from NGA-West2 database with the same parameters. A comparison in terms of Arias Intensity (AI), showed that stochastic ground motions reproduce accurately, on average, the AI shape; especially in range 0-75% of Arias intensity. A comparison in terms of AI range demonstrates that the AI dispersion is not completely reproduced, showing that a small part of variability is not taken into account by this predictive equation.

The absence of dependence on directivity effect expressed by two parameters showed that directivity effect must be taken into account in another way. The author's opinion is that the directivity effect is inside the overall distribution. In particular, we suggest that two distributions, corresponding two separate frequency ranges, in combination recreates the distribution studied in this paper. The two distributions should have different position and broadness; the distance between the two mean values should reproduce a directivity effect estimation.

5.3 Conditional scenario spectra through simulated spectra

The CSS is a set of response spectra with assigned rates of occurrence, which is able to recreate the seismic hazard of a case study. Rates of occurrence

are calibrated to match hazard obtained by probability seismic hazard assessment (PSHA). The application of CSS allows to build risk curves of engineering demand parameters (EDP); in other words, CSS provides an assessment of engineering application behavior in all seismic scenarios through a representative parameter (e.g. interstory drift). A set of Uniform hazard spectra with assigned hazard and the mean values of magnitude and distance for each level are inputs for CSS generation. The procedure can be divided in three steps.

First, ground motion prediction equations (GMPEs) are developed for each hazard level. Input parameters for GMPEs are mean values of magnitude and distance obtained by deaggregation. In case of GMPEs characterized by further parameters (e.g. soil category, fault mechanism), they can be set according to site condition.

Second, suites of at least 100 stochastic ground motions are generated from each GMPE. The employed methodology is based on Fourier amplitude spectrum model obtained by a target response spectrum (the GMPE in this case); the non-stationarity is achieved by the application of phase derivatives distribution predicted from magnitude, distance and soil category. Monte-carlo simulation random generates small sets of candidate scenario spectra; output of this simulation is a small set of spectra able to represent mean value, dispersion of all GMPEs and show correlation consistent with well-known models.

Third, rates of occurrence are assigned to all scenario spectra. Therefore, the rates are iteratively adjusted to match the input hazard by means of a misfit parameter. At the end of the process, spectra with a low rate of occurrence are removed, because their small contribution to the hazard.

Final result of this procedure is a set of spectra, which amount is less than one hundred. Compared to the method with recorded time histories, stochastic ground motions allows a remarkable reduction in the total number of spectra. The previous feature as well as the simplicity and speed of the procedure are the main advantages of the proposed methodology. Application of this CSS with engineering structure are expected in future studies.

Bibliography

- Aki K.* Scaling law of seismic spectrum // *Journal of Geophysical Research*. 1967. 72, 4. 1217–1231.
- Anderson J. G., Hough S. E.* A model for the shape of the Fourier amplitude spectrum of acceleration at high frequencies // *Bulletin of the Seismological Society of America*. 1984. 74, 5. 1969–1993.
- Arteta N. A.* C.A. METHODOLOGY BASED ON CONDITIONAL SCENARIO SPECTRA TO ESTIMATE ENGINEERING DEMAND PARAMETER RISK. 2017.
- Atkinson G. M., Assatourians K.* Implementation and validation of EXSIM (a stochastic finite-fault ground-motion simulation algorithm) on the SCEC broadband platform // *Seismological Research Letters*. 2015. 86, 1. 48–60.
- Atkinson G. M., Boore D. M.* Ground-motion relations for eastern North America // *Bulletin of the Seismological Society of America*. 1995. 85, 1. 17–30.
- B. Chiou N. Gregor R. Darragh, Silva W.* NGA project strong-motion database // *Earthquake Spectra*. 2008. 24, 1. 23–44.
- Baker J. W., Jayaram N.* Correlation of spectral acceleration values from NGA ground motion models // *Earthquake Spectra*. 2008. 24, 1. 299–317.
- Boore D. M.* Simulation of ground motion using the stochastic method // *Pure and Applied Geophysics*. 2003. 160, 3-4. 635–676.

- Campbell K. W., Bozorgnia Y.* NGA-West2 ground motion model for the average horizontal components of PGA, PGV, and 5 // *Earthquake Spectra*. 2014. 30, 3. 1087–1115.
- Carlton B., Abrahamson N.* Issues and approaches for implementing conditional mean spectra in practice // *Bulletin of the Seismological Society of America*. 2014. 104, 1. 503–512.
- Chiou B. S.-J., Youngs R. R.* Update of the Chiou and Youngs NGA model for the average horizontal component of peak ground motion and response spectra // *Earthquake Spectra*. 2014. 30, 3. 1117–1153.
- D. Ancheta Seyhan Silva Chiou Wooddell Graves Kottke Boore Kishida Donahue Stewart.* PEER NGA-West2 Database // *PEER Research Reports*. 2013.
- D. M. Boore C. Di Alessandro, Abrahamson N. A.* A generalization of the double-corner-frequency source spectral model and its use in the SCEC BBP Validation Exercise // *Bulletin of the Seismological Society of America*. 2014. 104, 5. 2387–2398.
- D. M. Boore E. Seyhan J. P. Stewart, Atkinson G. M.* NGA-West2 equations for predicting PGA, PGV, and 5shallow crustal earthquakes // *Earthquake Spectra*. 2014. 30, 3. 1057–1085.
- Douglas J., Aochi H.* A Survey of Techniques for Predicting Earthquake Ground Motions for Engineering Purposes // *Surveys in Geophysics*. 2008. 29, 3. 187–220.
- Gasparini D. A., Vanmarcke E. H. E. J.* *Simulated Earthquake Motions Compatible with Prescribed Response Spectra*. 1976.
- Idriss I.* An NGA-West2 empirical model for estimating the horizontal spectral values generated by shallow crustal earthquakes // *Earthquake Spectra*. 2014. 30, 3. 1155–1177.
- N. A. Abrahamson W. J. Silva, Kamai R.* Summary of the ASK14 ground motion relation for active crustal regions // *Earthquake Spectra*. 2014. 30, 3. 1025–1055.

- Ohsaki Y.* On the significance of phase content in earthquake ground motions // Earthquake Engineering and Structural Dynamics. 1979. 7, 5. 427–439.
- Sabetta F., Pugliese A.* Estimation of response spectra and simulation of nonstationary earthquake ground motions // Bulletin of the Seismological Society of America. 1996. 86, 2. 337–352.
- Saragoni G. Rodolfo, Hart G. C.* Simulation of artificial earthquakes // Earthquake Engineering and Structural Dynamics. 1973. 2, 3. 249–267.
- Stafford P. J.* Interfrequency Correlations among Fourier Spectral Ordinates and Implications for Stochastic Ground-Motion Simulation // Bulletin of the Seismological Society of America. 2017.
- T. Yokoyama N. Theofanopoulos, Watabe M.* Distribution of phase differences in relation to the earthquake magnitude, distance to the fault and local soil conditions // Proc. of 9th WCEE, Abstract. 1988. 1, A06-04. 55–55.
- Thráinsson H., Kiremidjian A. S.* Simulation of digital earthquake accelerograms using the inverse discrete Fourier transform // Earthquake engineering and structural dynamics. 2002. 31, 12. 2023–2048.
- Vamvatsikos D., Cornell C. A.* Incremental dynamic analysis // Earthquake Engineering and Structural Dynamics. 2002. 31, 3. 491–514.